Long-wavelength limit (homogenization) for two-dimensional photonic crystals

A. A. Krokhin,[1] P. Halevi,[2] and J. Arriaga[1]
[1]*Instituto de Física, Universidad Autónoma de Puebla, Apartado Postal J-48, Pue., 72570, Mexico*
[2]*Instituto Nacional de Astrofísica, Optica y Electrónica, Apartado Postal 51, Puebla, 72000, Mexico*
(Received 14 June 2001; published 7 March 2002)

Using the Fourier expansion method in the low-frequency limit we develop an effective-medium theory for two-dimensional (2D) periodic composites. We give a rigorous proof that, in this limit, a periodic medium behaves like a homogeneous one and we derive compact analytical formulas for the effective dielectric constants of a 2D photonic crystal, i.e., a periodic arrangement of infinite cylinders. These formulas are very general, namely the Bravais lattice, the cross-sectional form of cylinders, their filling fractions, and the dielectric constants are all arbitrary. So is the direction of propagation of the Bloch wave—out of plane in general, with special attention paid to the limiting cases of propagation in the plane of periodicity and parallel to the cylinders. In the latter case we report a behavior that is qualitatively different from that encountered in natural crystals and in 3D photonic crystals. Namely, for propagation along the cylinder axes, the wave fronts are not plane but rippled, with the distribution of the ripples following the pattern of the 2D Bravais lattice. We also demonstrate that the other long-wavelength optical properties can be described by means of the index ellipsoid. This allows us to apply the classification used in the optics of natural crystals (''crystal optics'') to photonic crystals. Namely, we characterize the photonic crystal entirely in terms of its three ''principal'' dielectric constants. One of these is associated with the direction parallel to the cylinders, and is given simply by the spatially averaged dielectric constant. For the two in-plane principal dielectric constants we derive three representations that are equivalent in principle, however, give rise to different rates of numerical convergence, depending on whether the dielectric constant or its reciprocal have been expanded in a Fourier series (respectively, ''ε representation'' and ''η representation''). Numerical results are given for a uniaxial (biaxial) photonic crystal with square (rectangular) lattice and circular cylinders. We conclude that for dielectric cylinders in air the η representation leads to much better convergence than the ε representation. The opposite holds for air cylinders in a dielectric. The accuracy is checked by applying Keller's theorems to conjugate structures.

DOI: 10.1103/PhysRevB.65.115208 PACS number(s): 42.70.Qs, 41.20.Jb, 42.25.Lc

I. INTRODUCTION

Control of light propagation by means of photonic crystal devices is mostly based on the idea of photonic band structure with a forbidden frequency band for the propagation of electromagnetic waves in the periodic composite. Photonic crystals which are used in waveguides, light emission devices, antenna substrates, etc., have wide enough band gaps, and just this property gives rise to the their numerous potential applications. The materials that the photonic crystals are fabricated from are mostly low-loss, high quality dielectrics with large contrast of the constituent materials. On the other hand, these artificial periodic composites can be also employed in the frequency region well below the gap, where the dispersion law is close to linear. Here the possible applications of photonic crystals as traditional optical elements like polarizers, prisms, and lenses were given very little consideration.[1,2] At the same time, in this long-wavelength regime the desirable optical characteristics of artificial periodic structures may be custom tailored by appropriate choices of the materials and the lattice geometry. These characteristics may be quite different from those of natural crystals and give rise, for instance, to unusually large birefringence.

In this paper we develop an analytic approach to the optical properties of two-dimensional (2D) photonic crystals. We are using the term ''optical'' in the sense that the wavelength of the propagating wave is much larger than the lattice period of the crystal; for natural crystals this condition fits the spectral region up to the ultraviolet.[3] For photonic crystals the lattice constant is, of course, a variable quantity. Therefore the long-wavelength regime's upper limit may be anywhere between radio waves and the far infrared. In practice, many photonic band gap materials exhibit a linear dispersion law, for both propagating modes, almost up to the gap frequency. This rather wide region (usually wider than the band-gap) can be considered as the domain of ''photonic crystal optics.'' Due to the linearity of the dispersion law, each mode is characterized by a unique parameter—its effective dielectric constant. It appears in the homogenized solution of Maxwell's equations for the periodic medium, which thus can be replaced by an effective homogeneous medium.

For a long time, there have been extensive efforts to construct effective-medium theories for inhomogeneous media. The well-known Maxwell-Garnett approximation[4] has been improved and generalized for diverse configurations, both periodic and disordered.[5–11] This phenomenological approach gives good results for very small filling fractions ($f \ll 1$ or $1-f \ll 1$) but it fails otherwise. It also does not take into account the microstructure of the inhomogeneous medium. Another approach, which is sensitive to the microstructure, concerns Maxwell's or Laplace's equation applied to periodic media.[12–18] This approach allows us to calculate parameters of the effective media with high accuracy, however, usually this requires rather hard numerical calculations. Recently a useful modification of the plane-wave expansion

method was proposed by Lalanne.[19] His numerical method permits us to calculate the parameters of the effective medium for intermediate filling fractions, and even at finite frequencies. However, it is restricted to a particular geometry of the inclusions, namely, when planes of permittivity discontinuities are parallel to the crystallographic axes of the photonic crystal.

A few mathematical theorems in the theory of homogenization permit making certain general conclusions about the effective medium and also checking the accuracy of the numerical calculations. It is worthwhile to mention the Hashin-Shtrikman[20] and Coriell-Jackson[21] limits, Keller's theorems for conjugate structures,[22,23] and the spectral representation.[24]

In the case of one-dimensional periodicity there are explicit analytical solutions for the dielectric constants of the effective medium. These are obtained by taking the limit $\omega,k\rightarrow 0$ of the dispersion relations for the TE and TM modes.[25] The effective medium for a 1D superlattice is a ''negative'' uniaxial crystal.[26] The 1D superlattice is the only case where the dispersion relation is known in analytical form for all frequencies, thanks to the simplicity of the Kronig-Penney model.[27] For periodicity in a plane (2D) or spatial (3D) periodicity, the plane-wave expansion method is widely used to calculate the band structure. For any finite Bloch wave-vector $\mathbf{k}$ the dispersion relation has an infinite number of solutions $\omega_n(\mathbf{k})$, where n is the band serial number. For $k\rightarrow 0$ (in the reduced Brillouin zone) all nonzero solutions $\omega_n(0)\neq 0$ correspond to an infinite number of optical modes which are irrelevant to the problem of homogenization. Two solutions with frequencies $\omega\rightarrow 0$ (and $k\rightarrow 0$) describe ''acoustic'' modes with two different polarizations; their finite slopes $\omega_{1,2}/k=c/\sqrt{\varepsilon_{eff}^{(1,2)}}$ determine the two effective dielectric constants for every direction of propagation. Due to this uniqueness, the acoustic modes can be investigated analytically by taking the limits $\omega,k\rightarrow 0$ in the characteristic equation. This approach has been proposed in Ref. 28 and later developed in Ref. 29 for 3D photonic crystals. The effective medium for 3D photonic crystals may be isotropic, uniaxial or biaxial,[29,30] depending on the symmetry of the lattice and that of the unit cell of the photonic crystal. A particularly compact result for the homogenization of 2D photonic crystals has been recently accomplished in Refs. 31,10,32, and 33. As we will see, for the 2D case, where the inclusions of the photonic crystal are infinitely long parallel rods, the effective medium is always birefringent, i.e., it is either uniaxial or biaxial; thus a specific feature of the 2D geometry is the impossibility of isotropy.[32] This can give rise to unusually large anisotropy[31] of 2D photonic crystals in comparison to natural crystals.

In this paper we derive the homogenized equations for arbitrary 2D photonic crystals and give the details of calculations which have been omitted in Refs. 31–33. The paper is organized as follows. In Sec. II we solve Maxwell's equations for the magnetic field in the low-frequency limit and in Sec. III obtain the two dielectric constants of the effective medium for propagation in the plane of periodicity; these describe the propagations of the ''ordinary'' and ''extraordinary'' waves. In Sec. IV we demonstrate that the long-wavelength optical properties of 2D photonic crystals can be described by the index ellipsoid,[3] namely, we derive the three principal dielectric constants in terms of the microstructure. In this section we also analyze different 2D Bravais lattices and different shapes of inclusions and make conclusions concerning optical symmetries of the corresponding photonic crystals. Section V is dedicated to the comparison with other works. Section VI contains results for propagation parallel to the axes of the cylinders. Here we solve the Maxwell equations for the displacement vector and derive two alternative representations for the principal dielectric constants. In Secs. VII and VIII we consider, respectively, the special cases of the rectangular and square lattices with circular cylinders. The accuracy of the numerical calculations is checked by Keller's theorem.[22,23] The conclusions are given in Sec. IX. Finally, we relegate the proofs of a few formulas to four appendixes.

II. MAXWELL'S EQUATIONS IN THE LOW-FREQUENCY LIMIT

We consider an inhomogeneous 3D medium with dielectric permittivity $\varepsilon(\mathbf{r})$. In a photonic crystal this function is periodic in space and so is the inverse dielectric function $\eta(\mathbf{r})=1/\varepsilon(\mathbf{r})$. The functions $\varepsilon(\mathbf{r})$ and $\eta(\mathbf{r})$ are given by the Fourier series

$$\varepsilon(\mathbf{r})=\sum_{\mathbf{G}}\ \varepsilon(\mathbf{G})\exp(i\mathbf{G}\cdot\mathbf{r}),\qquad \eta(\mathbf{r})=\sum_{\mathbf{G}}\ \eta(\mathbf{G})\exp(i\mathbf{G}\cdot\mathbf{r}),$$

$$\varepsilon(\mathbf{G})=\frac{1}{V_c}\int_{V_c}\varepsilon(\mathbf{r})\exp(-i\mathbf{G}\cdot\mathbf{r})d\mathbf{r},$$

$$\eta(\mathbf{G})=\frac{1}{V_c}\int_{V_c}\eta(\mathbf{r})\exp(-i\mathbf{G}\cdot r)d\mathbf{r}. \tag{1}$$

Here $\mathbf{G}$ are the reciprocal-lattice vectors and the integration runs over the unit cell with volume V_c. [Note that we are not restricted to the case of a periodic heterostructure where $\varepsilon(\mathbf{r})$ is a piecewise continuous function.] It is a simple matter to prove that

$$\sum_{\mathbf{G}''}\ \varepsilon(\mathbf{G}-\mathbf{G}'')\,\eta(\mathbf{G}''-\mathbf{G}')=\delta_{\mathbf{G},\mathbf{G}'}, \tag{2}$$

where $\delta_{\mathbf{G},\mathbf{G}'}$ is the Kronecker delta function. It follows that $\varepsilon(\mathbf{G},\mathbf{G}')$ and $\eta(\mathbf{G},\mathbf{G}')$ are mutually reciprocal matrices. That is, $\varepsilon^{-1}(\mathbf{G},\mathbf{G}')=\eta(\mathbf{G},\mathbf{G}')$ and $\eta^{-1}(\mathbf{G},\mathbf{G}')=\varepsilon(\mathbf{G},\mathbf{G}')$.

The wave equation for the monochromatic field $\mathbf{H}(\mathbf{r},t)=\mathbf{H}(\mathbf{r})\exp(-i\omega t)$ is written as follows:

$$\nabla\times[\,\eta(\mathbf{r})\nabla\times\mathbf{H}(\mathbf{r})]=\frac{\omega^2}{c^2}\mathbf{H}(\mathbf{r}). \tag{3}$$

In the periodic medium the Bloch theorem is applicable to $\mathbf{H}(\mathbf{r})$:

$$\mathbf{H}(\mathbf{r})=\exp(i\mathbf{k}\cdot\mathbf{r})\sum_{\mathbf{G}}\ \mathbf{h}_{\mathbf{k}}(\mathbf{G})\exp(i\mathbf{G}\cdot\mathbf{r}). \tag{4}$$

Using the transversality of the magnetic field,

$$(\mathbf{k}+\mathbf{G})\cdot\mathbf{h}_{\mathbf{k}}(\mathbf{G})=0, \tag{5}$$

a set of linear equations for the amplitudes $\mathbf{h}(\mathbf{G})$ is obtained:

$$\left(\frac{\omega^2}{c^2}-\overline{\eta}|\mathbf{k}+\mathbf{G}|^2\right)\mathbf{h}_{\mathbf{k}}(\mathbf{G}) = -\sum_{\mathbf{G}'\neq\mathbf{G}}\eta(\mathbf{G}-\mathbf{G}')(\mathbf{k}+\mathbf{G})\times[(\mathbf{k}+\mathbf{G}')\times\mathbf{h}_{\mathbf{k}}(\mathbf{G}')]. \tag{6}$$

Here

$$\overline{\eta}\equiv\eta(0)=\frac{1}{V_c}\int_{V_c}\eta(\mathbf{r})d\mathbf{r} \tag{7}$$

is the average inverse dielectric constant. For a binary composite $\overline{\eta}=f\eta_a+(1-f)\eta_b$, with $\eta_{a,b}=1/\varepsilon_{a,b}$, where ε_a and ε_b are the dielectric constants of the constituents and f is the filling fraction of material a. Our theory, however, is *not* restricted to binary composites.

Equation (6) is an infinite set of homogeneous linear equations for the eigenfunctions $\mathbf{h}_{\mathbf{k}}(\mathbf{G})$. The nontrivial solution is obtained by requiring that the determinant of the coefficients of $\mathbf{h}_{\mathbf{k}}(\mathbf{G})$ vanishes. This gives rise to the band structure $\omega=\omega_n(\mathbf{k})$, where n is the band index. Being an analytic function, $\omega_n(\mathbf{k})$ may be expanded in a power series of k (for any direction of $\mathbf{k}$) around $k=0$. For the lowest (acoustic) band of the spectrum $\omega(0)=0$ and the expansion starts from the linear term, i.e., $\omega(\mathbf{k})\propto k$. In the static limit $\omega\to 0$ there can be no magnetic field ($\mathbf{H}=0$). Therefore all Fourier coefficients $\mathbf{h}_{\mathbf{k}}(\mathbf{G})$ must vanish if $k\to 0$. The rates that they approach zero are different: the Fourier coefficients $\mathbf{h}_{\mathbf{k}}(\mathbf{G}\neq 0)$ vanish faster than the zero harmonic $\mathbf{h}_{\mathbf{k}}(\mathbf{G}=0)$. This follows from Eq. (6) if we substitute $\mathbf{G}=0$ in both sides and take the limit $k\to 0$,

$$\mathbf{h}_{\mathbf{k}}(\mathbf{G}=0)=-\frac{1}{\omega^2/c^2-\overline{\eta}k^2}\sum_{\mathbf{G}'\neq 0}\eta(-\mathbf{G}')\mathbf{k}\times[\mathbf{G}'\times\mathbf{h}_{\mathbf{k}}(\mathbf{G}')]. \tag{8}$$

Since the coefficients of $\mathbf{h}_{\mathbf{k}}(\mathbf{G}')$ are inversely proportional to k, all nonzero harmonics must approach zero at a higher rate than $\mathbf{h}_{\mathbf{k}}(0)$ does. Namely, $\mathbf{h}_{\mathbf{k}}(\mathbf{G}\neq 0)$ is of the same order as $\mathbf{h}_{\mathbf{k}}(0)kV_c^{1/3}$.

If the wavelength $\lambda=2\pi/k$ is much larger than the size of the unit cell, the inhomogeneous medium behaves like a homogeneous one. Equations (4), (6), and (8) form the mathematical basis for theory of homogenization of photonic crystals. Because, in this long-wavelength limit, $\mathbf{h}_{\mathbf{k}}(0)\gg\mathbf{h}_{\mathbf{k}}(\mathbf{G}\neq 0)$, the right-hand side (r.h.s.) of Eq. (4) reduces to the plane wave, i.e., the wave equation solution in a homogeneous medium,

$$\mathbf{H}(\mathbf{r})=\mathbf{h}_{\mathbf{k}}(0)\exp(i\mathbf{k}\cdot\mathbf{r}). \tag{9}$$

Moreover, because [according to Eq. (8)] $\mathbf{h}_{\mathbf{k}}(0)\perp\mathbf{k}$, this is a *transverse* plane wave. Terms with $\mathbf{G}\neq 0$ are corrections to this homogenized solution; the amplitudes $\mathbf{h}_{\mathbf{k}}(\mathbf{G})$ can be written as power series with respect to the small parameter $kV_c^{1/3}$. Thus our approach to the homogenization problem is essentially *quasistatic*; it is based on the asymptotic solution of Maxwell's equations. The static approach, based on the solution of the Laplace equation, has been developed in Ref. 34 (special case of a square lattice and circular cylinders) and later in Ref. 15 (arbitrary 3D structure).

The effective dielectric constant is defined as

$$\varepsilon_{eff}(\hat{\mathbf{k}})=\lim_{\omega,k\to 0}\left(\frac{kc}{\omega}\right)^2. \tag{10}$$

It turns out to be dependent not only on the average characteristics of the inhomogeneous medium, like $\overline{\varepsilon}$ or $\overline{\eta}$, but also on the details of microstructure, i.e., the geometry of the unit cell, the dielectric constants of the constituents, and the direction of propagation, $\hat{\mathbf{k}}=\mathbf{k}/k$.

From Faraday's Law for $\nabla\times\mathbf{H}$ it follows that $\mathbf{D}(\mathbf{r})=\sqrt{\varepsilon_{eff}}\mathbf{H}(\mathbf{r})\times\hat{\mathbf{k}}$. Then, by Eq. (9) the displacement vector $\mathbf{D}(\mathbf{r})$ is also a transverse plane wave. Further, from Faraday's Law we get that $\mathbf{H}(\mathbf{r})=\sqrt{\varepsilon_{eff}}\hat{\mathbf{k}}\times\mathbf{E}(\mathbf{r})$, so that $\mathbf{E}(\mathbf{r})$ is also a plane wave. However, while the electric field must lie in the plane perpendicular to $\mathbf{H}$ (the plane formed by the vectors $\mathbf{k}$ and $\mathbf{D}$), it is *not* a transverse wave. These conclusions are in accord with crystal optics.

Seemingly, the above analysis regarding the nature of the fields $\mathbf{H}(\mathbf{r})$, $\mathbf{D}(\mathbf{r})$, and $\mathbf{E}(\mathbf{r})$ holds for any direction of propagation $\hat{\mathbf{k}}$. Actually, it turns out that propagation parallel to the cylinders ($\hat{\mathbf{k}}=\hat{\mathbf{z}}$) is an exception.[35] Section VI will be devoted to this interesting case.

To calculate the limit in Eq. (10) one needs to derive the dispersion relation $\omega=\omega(\mathbf{k})$ which follows from the eigenvalue problem given by Eqs. (6) and (8). Keeping in Eq. (6) terms of the same order with respect to k, we get for $\mathbf{G}\neq 0$

$$\mathbf{h}_{\mathbf{k}}(\mathbf{G})=\frac{1}{\overline{\eta}G^2}\left\{\eta(\mathbf{G})\mathbf{G}\times[\mathbf{k}\times\mathbf{h}_{\mathbf{k}}(0)]+\sum_{\mathbf{G}'\neq\mathbf{G}}\eta(\mathbf{G}-\mathbf{G}')\mathbf{G}\times[\mathbf{G}'\times\mathbf{h}_{\mathbf{k}}(\mathbf{G}')]\right\}. \tag{11}$$

Now we substitute $\mathbf{h}_{\mathbf{k}}(0)$ from Eq. (8) into Eq. (11). Using Eqs. (5), (10), and (11), and introducing new variables,

$$\mathbf{a}_{\mathbf{k}}(\mathbf{G})=\mathbf{G}\times\mathbf{h}_{\mathbf{k}}(\mathbf{G}), \tag{12}$$

after some algebra (see Appendix A) we arrive at an infinite set of linear equations,

$$\mathbf{G}\times\left\{\sum_{\mathbf{G}'\neq 0}\eta(\mathbf{G}-\mathbf{G}')\mathbf{a}_{\mathbf{k}}(\mathbf{G}')-\frac{\eta(\mathbf{G})}{\varepsilon_{eff}^{-1}-\overline{\eta}}\sum_{\mathbf{G}'\neq 0}\eta(-\mathbf{G}')\hat{\mathbf{k}}\times[\hat{\mathbf{k}}\times\mathbf{a}_{\mathbf{k}}(\mathbf{G}')]\right\}=0. \quad (13)$$

It is seen that the coefficients of $\mathbf{a}_{\mathbf{k}}(\mathbf{G}')$ in Eq. (13) are now independent of the magnitude of $\mathbf{k}$. Hence, Eq. (13) is the homogenized Eq. (6), i.e., the long-wavelength limit $k\to 0$ has been accomplished.

Equation (13) is identically satisfied if the vector in the curly brackets is parallel to the vector $\mathbf{G}$, namely if

$$\sum_{\mathbf{G}'\neq 0}\eta(\mathbf{G}-\mathbf{G}')\mathbf{a}_{\mathbf{k}}(\mathbf{G}')-\frac{\eta(\mathbf{G})}{\varepsilon_{eff}^{-1}-\overline{\eta}}\sum_{\mathbf{G}'\neq 0}\eta(-\mathbf{G}')\hat{\mathbf{k}}\times[\hat{\mathbf{k}}\times\mathbf{a}_{\mathbf{k}}(\mathbf{G}')]=\alpha\mathbf{G}, \quad (14)$$

where α is a scalar. By Eq. (12), the vector $\mathbf{a}_{\mathbf{k}}(\mathbf{G})$ lies in the plane perpendicular to $\mathbf{G}$. In this plane it is given by the projections $a_1(\mathbf{G})$ and $a_2(\mathbf{G})$ on two orthogonal unit vectors $\hat{\mathbf{n}}_1(\mathbf{G})$ and $\hat{\mathbf{n}}_2(\mathbf{G})$ respectively, namely $\mathbf{a}(\mathbf{G})=a_1(\mathbf{G})\hat{\mathbf{n}}_1(\mathbf{G})+a_2(\mathbf{G})\hat{\mathbf{n}}_2(\mathbf{G})$. To get equations for the scalar quantities $a_1(\mathbf{G})$ and $a_2(\mathbf{G})$ we take projections of Eq. (14) on $\hat{\mathbf{n}}_1(\mathbf{G})$ and $\hat{\mathbf{n}}_2(\mathbf{G})$. Since $\mathbf{G}\cdot\hat{\mathbf{n}}_{1,2}(\mathbf{G})=0$, the right-hand sides of these equations are zeros and thus the indefinite scalar α disappears. The algebra simplifies with the use of the identity

$$[\hat{\mathbf{k}}\cdot\hat{\mathbf{n}}_{1,2}(\mathbf{G})][\hat{\mathbf{k}}\cdot\hat{\mathbf{n}}_{1,2}(\mathbf{G}')]-\hat{\mathbf{n}}_{1,2}(\mathbf{G})\cdot\hat{\mathbf{n}}_{1,2}(\mathbf{G}')=-[\hat{\mathbf{n}}_{1,2}(\mathbf{G})\times\hat{\mathbf{k}}]\cdot[\hat{\mathbf{n}}_{1,2}(\mathbf{G}')\times\hat{\mathbf{k}}]. \quad (15)$$

Then a set of equations for a_1 and a_2 can be written in a compact matrix form,

$$\sum_{\mathbf{G}'\neq 0}\left\{f_1(\mathbf{G},\mathbf{G}')\begin{pmatrix}\hat{\mathbf{n}}_1\cdot\hat{\mathbf{n}}_1' & \hat{\mathbf{n}}_1\cdot\hat{\mathbf{n}}_2'\\ \hat{\mathbf{n}}_2\cdot\hat{\mathbf{n}}_1' & \hat{\mathbf{n}}_2\cdot\hat{\mathbf{n}}_2'\end{pmatrix}+f_2(\mathbf{G},\mathbf{G}')\times\begin{pmatrix}(\hat{\mathbf{n}}_1\cdot\hat{\mathbf{k}})(\hat{\mathbf{k}}\cdot\hat{\mathbf{n}}_1') & (\hat{\mathbf{n}}_1\cdot\hat{\mathbf{k}})(\hat{\mathbf{k}}\cdot\hat{\mathbf{n}}_2')\\ (\hat{\mathbf{n}}_2\cdot\hat{\mathbf{k}})(\hat{\mathbf{k}}\cdot\hat{\mathbf{n}}_1') & (\hat{\mathbf{n}}_2\cdot\hat{\mathbf{k}})(\hat{\mathbf{k}}\cdot\hat{\mathbf{n}}_2')\end{pmatrix}\right\}\begin{pmatrix}a_1(\mathbf{G}')\\ a_2(\mathbf{G}')\end{pmatrix}=0. \quad (16)$$

Here $\hat{\mathbf{n}}_{1,2}'\equiv\hat{\mathbf{n}}_{1,2}(\mathbf{G}')$,

$$f_1(\mathbf{G},\mathbf{G}')=\eta(\mathbf{G}-\mathbf{G}')+(\varepsilon_{eff}^{-1}-\overline{\eta})^{-1}\eta(\mathbf{G})\eta(-\mathbf{G}'), \quad (17)$$

and

$$f_2(\mathbf{G},\mathbf{G}')=-(\varepsilon_{eff}^{-1}-\overline{\eta})^{-1}\eta(\mathbf{G})\eta(-\mathbf{G}'). \quad (18)$$

Equation (16) is applicable for any periodic 3D structure. The effective dielectric constant is determined from the condition of existence of nontrivial solutions of this set of homogeneous equations. Two different sets of linear equations were obtained in Ref. 29, using the wave equations for the electric and magnetic fields (E and H methods, respectively). Nevertheless, in spite of these differences of form, numerical results for the effective dielectric constants must be identical in the limit of an infinite number of plane waves ($\mathbf{G}$ values).

III. IN-PLANE EFFECTIVE DIELECTRIC CONSTANTS OF 2D PHOTONIC CRYSTALS

In what follows we limit the treatment to 2D periodicity, i.e., to a photonic crystal with infinitely long cylindrical inclusions. These may have any shape for their cross section and may form any 2D Bravais lattice. There may also be several cylinders in the unit cell.

Let the cylinders be parallel to the axis z, so the $x-y$ plane is the plane of periodicity. In this section we limit the propagation to the plane of periodicity, namely $k_z=0$. Then the vectors $\mathbf{G}=(G_x,G_y,0)$ and $\mathbf{k}=(k_x,k_y,0)$ have only two nonzero components. Remembering that $\hat{\mathbf{n}}_{1,2}\perp\mathbf{G}$, we choose the basic vector $\hat{\mathbf{n}}_1$ to be parallel to the axis z, namely $\hat{\mathbf{n}}_1=(0,0,1)$, and the basic vector $\hat{\mathbf{n}}_2$ is in the $x-y$ plane,

$$\hat{\mathbf{n}}_2=(-G_y/G,G_x/G,0). \quad (19)$$

The following identities hold:

$$\hat{\mathbf{k}}\cdot\hat{\mathbf{n}}_1=\hat{\mathbf{k}}\cdot\hat{\mathbf{n}}_1'=\hat{\mathbf{n}}_1\cdot\hat{\mathbf{n}}_2'=\hat{\mathbf{n}}_1'\cdot\hat{\mathbf{n}}_2=0,\quad \hat{\mathbf{n}}_1\cdot\hat{\mathbf{n}}_1'=1.$$

Then it follows from Eq. (16) that the equations for a_1 and a_2 are decoupled:

$$\sum_{\mathbf{G}'\neq 0}f_1(\mathbf{G},\mathbf{G}')a_1(\mathbf{G}')=0, \quad (20)$$

$$\sum_{\mathbf{G}'\neq 0}\{f_1(\mathbf{G},\mathbf{G}')(\hat{\mathbf{n}}_2\cdot\hat{\mathbf{n}}_2')+f_2(\mathbf{G},\mathbf{G}')(\hat{\mathbf{k}}\cdot\hat{\mathbf{n}}_2)(\hat{\mathbf{k}}\cdot\hat{\mathbf{n}}_2')\}a_2(\mathbf{G}')=0. \quad (21)$$

Equations (20) and (21) describe the TM or E mode ($\mathbf{E}\|\hat{\mathbf{z}}$) and the TE or H mode ($\mathbf{H}\|\hat{\mathbf{z}}$), respectively, as can be understood from Eq. (12) and the choice of the vectors $\hat{\mathbf{n}}_{1,2}$. For the case of propagation in the plane of periodicity these two modes are known to be decoupled for any frequency, not just in the long-wavelength limit.[36] Equations (20) and (21) have nonzero solutions if the corresponding determinants vanish,

$$\det_{\mathbf{G},\mathbf{G}'\neq 0}[(\varepsilon_{eff}^{-1}-\overline{\eta})\eta(\mathbf{G}-\mathbf{G}')+\eta(\mathbf{G})\eta(-\mathbf{G}')]=0,\quad E\text{ mode}, \quad (22)$$

$$\det_{\mathbf{G},\mathbf{G}'\neq 0}[(\varepsilon_{eff}^{-1}-\overline{\eta})\mathbf{G}\cdot\mathbf{G}'\,\eta(\mathbf{G}-\mathbf{G}')+(\hat{\mathbf{k}}\cdot\mathbf{G})(\hat{\mathbf{k}}\cdot\mathbf{G}')\eta(\mathbf{G})\eta(-\mathbf{G}')]=0,\quad H\text{ mode}. \quad (23)$$

To derive Eq. (23) from Eq. (21) we used the following identities:

$$\hat{\mathbf{n}}_2\cdot\hat{\mathbf{n}}_2'=\frac{\mathbf{G}\cdot\mathbf{G}'}{G\,G'},\quad \hat{\mathbf{n}}_2\cdot\hat{\mathbf{n}}_2'-(\hat{\mathbf{k}}\cdot\hat{\mathbf{n}}_2)(\hat{\mathbf{k}}\cdot\hat{\mathbf{n}}_2')=\frac{(\hat{\mathbf{k}}\cdot\mathbf{G})(\hat{\mathbf{k}}\cdot\mathbf{G}')}{G\,G'}.$$

Equations (22) and (23) determine the slopes of the acoustic branches, respectively, of the E and H modes, that is—according to Eq. (10)—the effective dielectric constants for these modes. These equations are polynomials of infinite order in $(\varepsilon_{eff}^{-1}-\overline{\eta})$. Below we show that each of them has a single physical solution.

To reduce Eq. (22) to a standard eigenvalue problem we multiply it from the right by $\det_{\mathbf{G},\mathbf{G}'\neq 0}[\varepsilon(\mathbf{G}-\mathbf{G}')]$ and use the identity $\det A\det B=\det AB$. We also make use of the fact that $\varepsilon(\mathbf{G}-\mathbf{G}')$ and $\eta(\mathbf{G}-\mathbf{G}')$ are, according to Eq. (2), mutually reciprocal matrices and hence satisfy the identity

$$\sum_{\mathbf{G}''}\eta(\mathbf{G}-\mathbf{G}'')\varepsilon(\mathbf{G}''-\mathbf{G}')\equiv\sum_{\mathbf{G}''\neq 0}\eta(\mathbf{G}-\mathbf{G}'')\varepsilon(\mathbf{G}''-\mathbf{G}')+\eta(\mathbf{G})\varepsilon(-\mathbf{G}')=\delta_{\mathbf{G}\mathbf{G}'},\tag{24}$$

and its special case for $\mathbf{G}=0$,

$$\sum_{\mathbf{G}''\neq 0}\eta(-\mathbf{G}'')\varepsilon(\mathbf{G}''-\mathbf{G}')+\overline{\eta}\varepsilon(-\mathbf{G}')=\delta_{\mathbf{G}'0}.\tag{25}$$

Then Eq. (22) takes the form of the standard eigenvalue problem,

$$\det_{\mathbf{G},\mathbf{G}'\neq 0}[\eta(\mathbf{G})\varepsilon(-\mathbf{G}')-\lambda\delta_{\mathbf{G}\mathbf{G}'}]=0,\quad \lambda=1-\varepsilon_{eff}\overline{\eta}.\tag{26}$$

Expanding the determinant we get

$$\det_{\mathbf{G},\mathbf{G}'\neq 0}[\eta(\mathbf{G})\varepsilon(-\mathbf{G}')-\lambda\delta_{\mathbf{G}\mathbf{G}'}]=\lim_{n\to\infty}(-1)^n(\lambda^n+\alpha_1\lambda^{n-1}+\cdots+\alpha_n).\tag{27}$$

The polynomial on the right-hand side is the characteristic polynomial of the matrix

$$C(\mathbf{G},\mathbf{G}')=\eta(\mathbf{G})\varepsilon(-\mathbf{G}'),\quad \mathbf{G},\mathbf{G}'\neq 0.\tag{28}$$

The coefficients of the characteristic polynomial of any matrix C can be obtained by using the recurrence relation,[37]

$$\alpha_1=-\operatorname{Tr}C(\mathbf{G},\mathbf{G}'),$$

$$\alpha_2=-\frac{1}{2}\operatorname{Tr}(C^2+\alpha_1 C)=-\frac{1}{2}[\operatorname{Tr}(C^2)-(\operatorname{Tr}C)^2],\tag{29}$$

$$\cdots$$

$$\alpha_n=-\frac{1}{n}\operatorname{Tr}(C^n+\alpha_1 C^{n-1}+\cdots+\alpha_{n-1}C).$$

Here, the trace is taken over all diagonal elements except $\mathbf{G}=\mathbf{G}'=0$. Now, due to the separation of the variables $\mathbf{G}$ and $\mathbf{G}'$ in the matrix $C(\mathbf{G},\mathbf{G}')$ [Eq. (28)], the trace has the property

$$\operatorname{Tr}(C^n)=\operatorname{Tr}C\operatorname{Tr}(C^{n-1}).\tag{30}$$

This ensures that all the coefficients $\alpha_n=0$ for $n=2,3,\ldots,$ as can be proved by mathematical induction, see Appendix B. Now Eq. (26) is rewritten in a simple form,

$$\det_{\mathbf{G},\mathbf{G}'\neq 0}[\eta(\mathbf{G})\varepsilon(-\mathbf{G}')-\lambda\delta_{\mathbf{G}\mathbf{G}'}]=\lim_{n\to\infty}(-1)^n\lambda^{n-1}(\lambda+\alpha_1)=0.\tag{31}$$

The infinitely degenerate root $\lambda=0$ is not a solution of Eq. (26). Hence Eq. (31) has the unique (nonzero) solution $\lambda=-\alpha_1$. Then, using Eqs. (26), (29), (28), and (24) (for $\mathbf{G}=\mathbf{G}'=0$), we get that

$$1-\varepsilon_{eff}\overline{\eta}=\sum_{\mathbf{G}\neq 0}\eta(\mathbf{G})\varepsilon(-\mathbf{G})=\sum_{\mathbf{G}}\eta(\mathbf{G})\varepsilon(-\mathbf{G})-\varepsilon(0)\eta(0)=1-\overline{\varepsilon\eta}.\tag{32}$$

Comparison of the first and the last expressions yields the effective dielectric constant for the E mode, namely

$$\varepsilon_E=\overline{\varepsilon}.\tag{33}$$

This effective dielectric constant is thus independent of the direction of propagation and it is simply the weighted average dielectric constant. This result is in fact known to be valid not only for periodic systems, but also for any inhomogeneous dielectric with dielectric constant $\varepsilon(\mathbf{r})$ that is independent of the coordinate z (see, e.g., Ref. 24).

Now let us turn to the dispersion relation Eq. (23) for the H mode. Multiplying this equation by $\det\{[\mathbf{G}\cdot\mathbf{G}'\eta(\mathbf{G}-\mathbf{G}')]^{-1}\}$ we get a standard eigenvalue problem,

$$\det_{\mathbf{G},\mathbf{G}'\neq 0}[B(\mathbf{G},\mathbf{G}')-\Lambda\delta_{\mathbf{G}\mathbf{G}'}]=0,\quad \Lambda=1/\varepsilon_{eff}-\overline{\eta},\tag{34}$$

where

$$B(\mathbf{G},\mathbf{G}')=-\hat{\mathbf{k}}\cdot\mathbf{G}\,\eta(\mathbf{G})\sum_{\mathbf{G}''\neq 0}\hat{\mathbf{k}}\cdot\mathbf{G}''\,\eta(-\mathbf{G}'')\times[\mathbf{G}''\cdot\mathbf{G}'\,\eta(\mathbf{G}''-\mathbf{G}')]^{-1},\quad \mathbf{G},\mathbf{G}'\neq 0.\tag{35}$$

Here $[\cdots]^{-1}$ implies inversion of the matrix in the brackets. The matrix $B(\mathbf{G},\mathbf{G}')$ is written in a form similar to the matrix $C(\mathbf{G},\mathbf{G}')$ in Eq. (28), namely as a product of two factors, one of which depends only on $\mathbf{G}$ and the other only on $\mathbf{G}'$. Then it is clear that Eq. (30) also holds for the matrix B, and that the procedure in Eqs. (27)–(31) carries over for the case at hand. The only nonzero coefficient of its characteristic polynomial is $\alpha_1=-\operatorname{Tr}B(\mathbf{G},\mathbf{G}')$ and then $\Lambda\equiv 1/\varepsilon_{eff}-\overline{\eta}=-\alpha_1$. This results in the effective dielectric constant for the H polarization,

$$\varepsilon_H(\hat{\mathbf{k}}) = \frac{1}{\overline{\eta} + \mathrm{Tr}\, B(\mathbf{G},\mathbf{G}')}, \tag{36}$$

or

$$\varepsilon_H(\hat{\mathbf{k}}) = 1 \Big/ \left\{ \overline{\eta} - \sum_{\mathbf{G},\mathbf{G}' \neq 0} \hat{\mathbf{k}}\cdot\mathbf{G}\hat{\mathbf{k}}\cdot\mathbf{G}'\, \eta(\mathbf{G})\, \eta(-\mathbf{G}') \times [\mathbf{G}\cdot\mathbf{G}'\, \eta(\mathbf{G}-\mathbf{G}')]^{-1} \right\}. \tag{37}$$

This effective dielectric constant depends on the direction of propagation in the $x-y$ plane and on the details of the photonic crystal structure. For propagation in the plane of periodicity, Eqs. (33) and (37) give a complete solution for the effective dielectric constants of *any* 2D photonic crystal in the low-frequency limit. In what follows we will show how to calculate the *principal dielectric constants*, which give the customary description for anisotropic media in crystal optics.[3]

IV. UNIAXIAL AND BIAXIAL PHOTONIC CRYSTALS

The angular dependence of $\varepsilon_H(\hat{\mathbf{k}})$ in Eq. (36) can be obtained explicitly for an arbitrary 2D periodic structure. In the $x-y$ plane we introduce a polar angle φ, measured from the x axis, taken in an arbitrary direction. Substituting $\hat{\mathbf{k}} = (\cos\varphi, \sin\varphi)$ in Eq. (35) and calculating the trace of the matrix $B(\mathbf{G},\mathbf{G}')$, we get

$$\frac{1}{\varepsilon_H(\varphi)} = (\overline{\eta} - A_{xx})\cos^2\varphi + (\overline{\eta} - A_{yy})\sin^2\varphi - A_{xy}\sin 2\varphi. \tag{38}$$

Here

$$A_{ik} = \frac{1}{2} \sum_{\mathbf{G},\mathbf{G}' \neq 0} (G_i G_k' + G_k G_i')\, \eta(\mathbf{G}) \times \eta(-\mathbf{G}')[\mathbf{G}\cdot\mathbf{G}'\, \eta(\mathbf{G}'-\mathbf{G})]^{-1}, \quad i,k = x,y. \tag{39}$$

Equation (38) describes a rotated ellipse in polar coordinates (ρ,φ), where the radius is $\rho(\varphi) = \sqrt{\varepsilon_H(\varphi)}$. Hence we come to the conclusion that the values of the effective refractive index $n_H(\varphi) \equiv \sqrt{\varepsilon_H(\varphi)}$ lie on this ellipse. Such a behavior is well known in the optics of natural crystals and allows us to introduce the index ellipsoid.[3] The axes of the index ellipsoid (x_0, y_0, z_0) are three mutually orthogonal directions along which the vectors **D** and **E** are parallel to each other.

For 2D photonic crystals one of these axes (z_0) is necessarily parallel to the z-axis, because for the E-polarized mode $\mathbf{D}(\mathbf{r}) \| \mathbf{E}(\mathbf{r}) \| \hat{\mathbf{z}}$. Thus the other two principal axes are in the plane of periodicity. The index ellipsoid is given by the equation[3,38]

$$\frac{x_0^2}{\varepsilon_1} + \frac{y_0^2}{\varepsilon_2} + \frac{z_0^2}{\varepsilon_3} = 1, \tag{40}$$

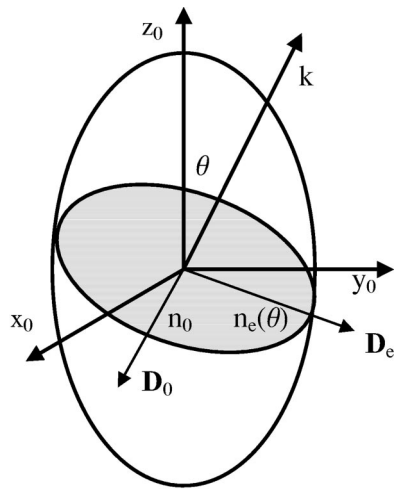

FIG. 1. The index ellipsoid (general case) and the determination of the ordinary and extraordinary refractive indices and corresponding displacement vectors of a *uniaxial* material for a given direction of the wave vector **k** (see Sec. IV).

where ε_1, ε_2, and ε_3 are the *principal dielectric constants*. For every direction of propagation $\hat{\mathbf{k}}$ the index ellipsoid determines two refractive indices. They are, simply, the lengths of the semiaxes of the ellipse which is obtained by cutting the index ellipsoid by a plane through its center and that is perpendicular to $\hat{\mathbf{k}}$, see Fig. 1. Also, the directions of these semiaxes coincide with the directions of the displacement vectors **D** of the corresponding modes. If $\hat{\mathbf{k}}$ is in the $x-y$ plane, then one of the semiaxes of the aforementioned ellipse coincides with the z axis. Then one propagating mode is characterized by $\mathbf{D} \| \hat{\mathbf{z}}$ and, according to Eq. (40), the vertical semiaxis length is $\sqrt{\varepsilon_3}$, independent of the direction $\hat{\mathbf{k}}$. As pointed out before, this is just the E mode, whose effective dielectric constant has been determined by Eq. (33). Hence we can make the identification

$$\varepsilon_3 = \overline{\varepsilon}, \tag{41}$$

thus having determined one of the principal dielectric constants in Eq. (40).

The displacement vector and hence electric field of the other propagating mode is parallel to the plane of periodicity, so this is, obviously, the H mode. Now, the effective dielectric constant depends on the angle φ_0 between $\hat{\mathbf{k}}$ and the x_0 axis. By expressing the ellipse $z_0 = 0$ of Eq. (40) in polar coordinites, simple geometry (see Fig. 1) yields the following expression for the horizontal semiaxis of the index ellipsoid:

$$\frac{1}{\varepsilon_H(\varphi_0)} = \frac{\sin^2\varphi_0}{\varepsilon_1} + \frac{\cos^2\varphi_0}{\varepsilon_2}. \tag{42}$$

This equation gives ε_H in the form of an ellipse expressed in its proper axes system (polar representation). Clearly, Eq. (38) describes the same ellipse, however, expressed with respect to some arbitrarily chosen axes x,y. Rotating the axes x,y by an angle $\theta = \varphi_0 - \varphi$ we can diagonalize the tensor

A_{ik}. The angle θ is obtained from the condition that the nondiagonal term, which is proportional to $\sin 2\varphi_0$, vanishes:

$$\tan 2\theta = \frac{2A_{xy}}{A_{yy} - A_{xx}}. \tag{43}$$

This formula determines the directions of the principal crystalline axes with respect to some (initially) arbitrarily chosen axes. Of course, in simple cases (such as a rectangular Bravais lattice) the directions of the principal axes are intuitively obvious. Then one chooses, from the outset, $x = x_0$ and $y = y_0$, so that A_{xy} will turn out to vanish.

Furthermore, the coefficients of the terms $\sin^2 \varphi_0$ and $\cos^2 \varphi_0$ of the rotated ellipse (38) determine the principal dielectric constants ε_1 and ε_2 in Eq. (42) as

$$\varepsilon_1 = (\overline{\eta} - A_{xx} \sin^2 \theta - A_{yy} \cos^2 \theta - A_{xy} \sin 2\theta)^{-1}, \tag{44}$$

$$\varepsilon_2 = (\overline{\eta} - A_{xx} \cos^2 \theta - A_{yy} \sin^2 \theta + A_{xy} \sin 2\theta)^{-1}. \tag{45}$$

It is the symmetry of the unit cell that determines whether a photonic crystal is uniaxial ($\varepsilon_1 = \varepsilon_2$) or biaxial ($\varepsilon_1 \neq \varepsilon_2$). Unlike 3D photonic crystals, 2D crystals cannot be isotropic ($\varepsilon_1 = \varepsilon_2 = \varepsilon_3$). This property is guaranteed by the Wiener bounds ($\varepsilon_{1,2} < \varepsilon_3$) valid at least for in-plane isotropy, namely $\varepsilon_1 = \varepsilon_2$.[39] If the crystal possesses a third- or higher-order rotational axis z, then any second-rank symmetric tensor such as A_{ik} ($i,k = x,y$), Eq. (39), is reduced to a scalar,[38] $A_{ik} = A\delta_{ik}$. Then Eqs. (44), (45), and (39) may be simplified as

$$\varepsilon_1 = \varepsilon_2 = (\overline{\eta} - A)^{-1} = \left\{ \overline{\eta} - \frac{1}{2} \sum_{\mathbf{G},\mathbf{G}' \neq 0} \mathbf{G} \cdot \mathbf{G}' \, \eta(\mathbf{G}) \, \eta(-\mathbf{G}') \times [\mathbf{G} \cdot \mathbf{G}' \, \eta(\mathbf{G}' - \mathbf{G})]^{-1} \right\}^{-1}. \tag{46}$$

Here $[\cdots]^{-1}$ implies matrix inversion, while $\{\cdots\}^{-1}$ means "reciprocal." This compact formula gives the principal dielectric constant (associated with the plane of periodicity) of a uniaxial photonic crystal. The optical axis coincides with the axis z, which is to say that birefringence is absent for a single direction of propagation—the direction parallel to the cylinders. For propagation in this direction (with $\mathbf{E} \perp \hat{\mathbf{z}}$) the phase velocities of the "ordinary" and "extraordinary" waves are the same, $\omega/k = c/\sqrt{\varepsilon_1}$, with ε_1 given by Eq. (46). Of course, for any direction of propagation the ordinary wave propagates with the same speed, $c/\sqrt{\varepsilon_1}$, by definition. Because this velocity is always greater than the velocity $c/\sqrt{\varepsilon_3}$ of the extraordinary wave (with $\mathbf{E} \| \hat{\mathbf{z}}$) that propagates in the plane of periodicity, we may conclude that uniaxial 2D photonic crystals are necessarily "negative"—just like 1D superlattices.

For artificial periodic structures the symmetry of the unit cell is determined by both the symmetry of the Bravais lattice and the symmetry of the inclusions. Being macroscopic, the latter may possess a symmetry that is lower than that of the lattice. For 3D periodicity this situation has been studied in Ref. 40. Namely, spherical inclusions with anisotropic dielectric constants in an fcc lattice give rise to the splitting of the dispersion curves for two polarizations in the low-frequency limit, thus breaking the isotropy of the photonic crystal. For 2D photonic crystals, there can be only limited isotropy—in the $(x-y)$ plane. The following structures (with third- or higher-order rotational axis) exhibit such isotropy: the square lattice with circular or square cylinders and the hexagonal lattice with circular or with equilateral triangular cylinders. The unit cells of these structures are shown in Fig. 2; they all correspond to uniaxial 2D photonic crystals. A few examples of unit cells that exhibit anisotropy in the plane of periodicity are given in Fig. 3. These unit cells define biaxial 2D photonic crystals.

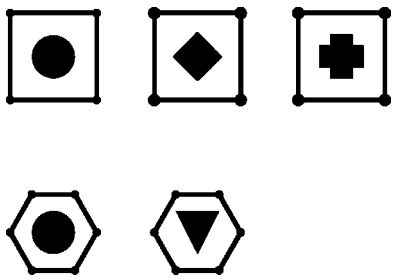

FIG. 2. Examples of unit cells of 2D photonic crystals that exhibit isotropy in the plane of periodicity; the corresponding photonic crystals are optically uniaxial. Note that photonic crystals that have a rectangular or an oblique (general) 2D Bravias lattice cannot be uniaxial.

The Eqs. (44), (45), and (41) specify, completely and compactly, the principal dielectric constants of an arbitrary 2D photonic crystal. They are expressed in terms of the geometry of the unit cell and the dielectric constants of the constituent materials. If ε_1, ε_2, and ε_3 are known, then,

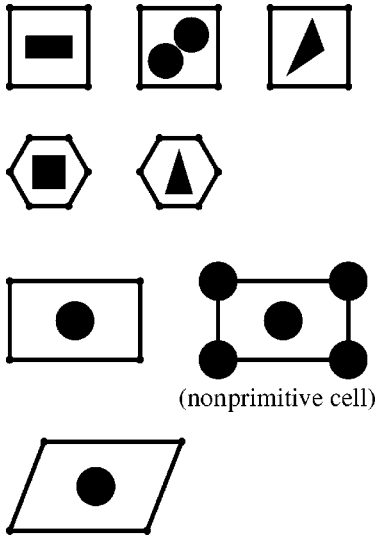

FIG. 3. Examples of unit cells of 2D photonic crystals that are anisotropic in the plane of periodicity; the corresponding photonic crystals are biaxial. In these examples, either the inclusions or the lattice is anisotropic in the plane of periodicity.

using formulas of crystal optics,[3,38] the propagation constants can be readily calculated for any direction of $\hat{\mathbf{k}}$.

V. COMPARISON WITH OTHER WORKS

There are two analytic studies of the problem of homogenization where the final result for the effective dielectric constant is expressed in terms of $\varepsilon(\mathbf{G})$. One has been proposed by Datta *et al.*[29] for 3D photonic crystals and then reduced by Kirchner *et al.*[10] to the special case of 2D periodicity. Their approach is a quasistatic one, namely, the effective dielectric constant is obtained by taking the limit (10). Another approach (static), based on the solution of Laplace's equation was developed by Bergman and Dunn.[15]

The method described in Secs. II and III, being quasistatic, is closer to the approach of Datta *et al.*[29] Rewriting Eqs. (C12)–(C16) of Kirchner *et al.*[10] in our notation we get

$$\varepsilon_H(\hat{\mathbf{k}})=\overline{\varepsilon}-\sum_{\mathbf{G},\mathbf{G}'\neq 0}\mathbf{p_k}\cdot\mathbf{G}\mathbf{p_k}\cdot\mathbf{G}'\varepsilon(\mathbf{G})\varepsilon(-\mathbf{G}')\times[\mathbf{G}\cdot\mathbf{G}'\varepsilon(\mathbf{G}'-\mathbf{G})]^{-1}. \tag{47}$$

Here $\mathbf{p_k}$ is a unit vector in the plane of periodicity and perpendicular to $\mathbf{k}$. While the structure of Eq. (47) is not unlike the structure of Eq. (37), the two representations for the effective dielectric constant are different. Equation (47) was obtained from the wave equation for the electric field, while Eq. (37) follows from the wave equation (3) for the magnetic field. Since the spectrum of Maxwell's equations for a given structure is unique, these two representations must be equivalent. This means that the following identity should hold:

$$\left\{\overline{\varepsilon}-\sum_{\mathbf{G},\mathbf{G}'\neq 0}\mathbf{p_k}\cdot\mathbf{G}\mathbf{p_k}\cdot\mathbf{G}'\varepsilon(\mathbf{G})\varepsilon(-\mathbf{G}')\times[\mathbf{G}\cdot\mathbf{G}'\varepsilon(\mathbf{G}'-\mathbf{G})]^{-1}\right\}\left\{\overline{\eta}-\sum_{\mathbf{G},\mathbf{G}'\neq 0}\hat{\mathbf{k}}\cdot\mathbf{G}\hat{\mathbf{k}}\cdot\mathbf{G}'\eta(\mathbf{G})\eta(-\mathbf{G}')[\mathbf{G}\cdot\mathbf{G}'\eta(\mathbf{G}'-\mathbf{G})]^{-1}\right\}=1. \tag{48}$$

Each factor in the curly brackets depends on the direction of the vector $\mathbf{k}$, but the product is independent of it. It is clear that this identity is related to Eq. (2), however, an analytic proof seems to be difficult. Instead, we opt for a numerical demonstration. In Fig. 4 we plot the left-hand side of Eq. (48) as a function of the angle $\varphi(\hat{\mathbf{k}},\hat{\mathbf{x}})$ (solid line) for a 2D periodic crystal with rectangular lattice and circular cylinders. The unit cell is taken to be strongly anisotropic, with ratio of the sides 1:5. This structure exhibits strong birefringence, i.e., the factors in Eq. (48) vary substantially with φ (dotted and dashed curves in Fig. 4). Nevertheless, the product of these factors is practically independent of φ and is very close to 1. This gives numerical evidence of the identity (48).

Now we will show that the result obtained by Bergman and Dunn[15] by means of an electrostatic approach can be also written in the form of Eq. (47).[41] In this approach the effective dielectric constant $\varepsilon_{eff}(\hat{\mathbf{E}})$ is obtained as a function of the direction of the dc electric field, $\hat{\mathbf{E}}=\mathbf{E}/E$. Using Eqs. (2.5) and (2.26) of Ref. 15 one obtains

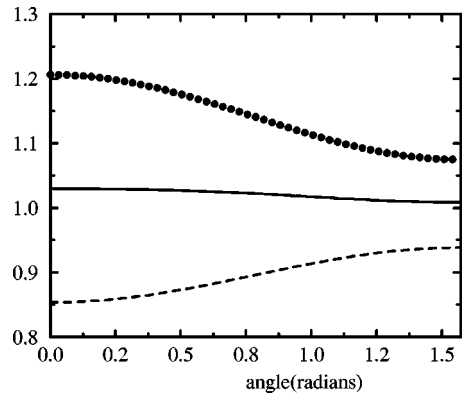

FIG. 4. Numerical evidence of the identity (48) for a rectangular lattice with sides ratio $a/b=5$ and circular cylinders with filling fraction $f=0.05$ and dielectric constant $\varepsilon_a=20$. The solid line shows the left-hand side of Eq. (48), and the dotted and dashed lines show the first and second factors in curly brackets. The number of plane waves used in the calculations is $N=1636$. These curves are plotted as a function of the angle between the wave vector $\mathbf{k}$ and one of the basis vectors of the (rectangular) unit cell.

$$\frac{\varepsilon_b-\varepsilon_{eff}(\hat{\mathbf{E}})}{\varepsilon_b-\varepsilon_a}-f=\sum_{\mathbf{G}\neq 0}\hat{\mathbf{E}}\cdot\mathbf{G}\theta_{-\mathbf{G}}a_{\mathbf{G}}. \tag{49}$$

Here $\theta_{\mathbf{G}}=\varepsilon(\mathbf{G})/(\varepsilon_a-\varepsilon_b)$, $\theta_{\mathbf{G}=0}=f$. The formal solution for $a_{\mathbf{G}}$ follows from Eq. (2.23),

$$a_{\mathbf{G}}=\sum_{\mathbf{G}'\neq 0}(s-\Gamma)^{-1}_{\mathbf{G},\mathbf{G}'}\hat{\mathbf{E}}\cdot\mathbf{G}'\theta_{\mathbf{G}'}, \tag{50}$$

where $s=\varepsilon_b/(\varepsilon_b-\varepsilon_a)$ and the nondiagonal matrix elements of the operator Γ are given by Eq. (2.21) of Ref. 15,

$$\Gamma_{\mathbf{G},\mathbf{G}'}=\mathbf{G}\cdot\mathbf{G}'\theta(\mathbf{G}-\mathbf{G}'),\quad \mathbf{G}\neq\mathbf{G}'. \tag{51}$$

The diagonal matrix elements are independent on $\mathbf{G}$ and equal to $\Gamma_{\mathbf{G},\mathbf{G}}=f$. Combining Eqs. (49)–(51) we get

$$\varepsilon_{eff}(\hat{\mathbf{E}})-\overline{\varepsilon}=\sum_{\mathbf{G}\neq 0}\hat{\mathbf{E}}\cdot\mathbf{G}\varepsilon(-\mathbf{G})a_{\mathbf{G}}=\sum_{\mathbf{G},\mathbf{G}'\neq 0}\frac{\hat{\mathbf{E}}\cdot\mathbf{G}\varepsilon(-\mathbf{G})(s-\Gamma)^{-1}_{\mathbf{G},\mathbf{G}'}\hat{\mathbf{E}}\cdot\mathbf{G}'\varepsilon(\mathbf{G}')}{GG'(\varepsilon_a-\varepsilon_b)}. \tag{52}$$

A direct comparison of the diagonal and nondiagonal matrix elements shows that the operator $(s-\Gamma)$ can be written as follows:

$$s\delta_{\mathbf{G},\mathbf{G}'}-\Gamma_{\mathbf{G},\mathbf{G}'}\equiv-\frac{\mathbf{G}\cdot\mathbf{G}'\varepsilon(\mathbf{G}-\mathbf{G}')}{GG'(\varepsilon_a-\varepsilon_b)}. \tag{53}$$

Substitution of Eq. (53) into Eq. (52) gives the effective dielectric constant for a given direction of the electric field,

$$\varepsilon_{eff}(\hat{\mathbf{E}})=\overline{\varepsilon}-\sum_{\mathbf{G},\mathbf{G}'\neq 0}\hat{\mathbf{E}}\cdot\mathbf{G}\hat{\mathbf{E}}\cdot\mathbf{G}'\varepsilon(\mathbf{G})\varepsilon(-\mathbf{G}')\times[\mathbf{G}\cdot\mathbf{G}'\varepsilon(\mathbf{G}'-\mathbf{G})]^{-1}. \tag{54}$$

In the low-frequency limit the electric field $\mathbf{E}$ of the H mode lies in the plane of periodicity perpendicular to $\hat{\mathbf{k}}$, i.e., the vector $\hat{\mathbf{E}}=\mathbf{E}/E$ coincides with the vector $\mathbf{p}_\mathbf{k}$ in Eq. (47). Therefore Eq. (54) gives the effective dielectric constant for the H-mode propagating in the direction $\hat{\mathbf{k}}$ ($\hat{\mathbf{k}}\perp\hat{\mathbf{E}}$), provided that $\hat{\mathbf{E}}$ is replaced by $\mathbf{p}_\mathbf{k}$. After this replacement Eq. (54) becomes identical to Eq. (47), and both equations are equivalent to Eq. (37).

VI. PROPAGATION PARALLEL TO THE CYLINDERS AXES

Along the cylinder axes the medium is translationally invariant, and therefore the Bloch vector is replaced by the ordinary wave vector $\mathbf{k}=(0,0,k)$. Then k is not bounded any more by the Brillouin zone and the dispersion law in the z direction does not reveal a band structure. As a result, gaps cannot appear in the frequency spectrum.

In a uniaxial crystal both eigenmodes propagating along the optical axis (the z axis) have equal phase velocities $c/\sqrt{\varepsilon}_1$, where ε_1 is given by Eq. (46). If the crystal is biaxial, the eigenmodes propagate with different velocities, $c/\sqrt{\varepsilon}_1$ and $c/\sqrt{\varepsilon}_2$, where ε_1 and ε_2 are given by Eqs. (44) and (45). In this section we will study the structure of the electromagnetic field for the modes propagating along the axis z. The procedure of homogenization at low frequencies also has some specific features, which we will describe by taking the limits $\omega,k\to 0$ of the characteristic equation for the displacement field $\mathbf{D}$. It turns out that this leads to a representation for the principal dielectric constants $\epsilon_{1,2}$ that is formally different from Eqs. (44) and (45). The formulas obtained by the H and the D methods have different rates of convergence. This will allow us to device a numerical method that leads to improved accuracy of the results.

It can be readily proved that the eigenequation for the Fourier components of the displacement field $\mathbf{d}_\mathbf{k}(\mathbf{G})$ has the following form:

$$\frac{\omega^2}{c^2}\mathbf{d}_\mathbf{k}(\mathbf{G})=\sum_{\mathbf{G}'}\eta(\mathbf{G}-\mathbf{G}')[|\mathbf{k}+\mathbf{G}|^2\mathbf{d}_\mathbf{k}(\mathbf{G}')-(\mathbf{k}+\mathbf{G})(\mathbf{k}+\mathbf{G})\cdot\mathbf{d}_\mathbf{k}(\mathbf{G}')]. \tag{55}$$

For the case $\mathbf{k}=k\hat{\mathbf{z}}$ (i.e., $\mathbf{k}\perp\mathbf{G}$ and $|\mathbf{k}+\mathbf{G}|^2=k^2+G^2$) the vector $\mathbf{d}_\mathbf{k}(\mathbf{G})$ has a longitudinal component $d_z(\mathbf{G})$ which yields the equation

$$\frac{\omega^2}{c^2}d_z(\mathbf{G})=\sum_{\mathbf{G}'}\eta(\mathbf{G}-\mathbf{G}')[G^2d_z(\mathbf{G}')-k\mathbf{G}\cdot\mathbf{d}_\perp(\mathbf{G}')]. \tag{56}$$

In the low-frequency limit $\omega\to 0$ this longitudinal component approaches zero since, for $\omega=0$ and $k=0$, Eq. (56) has only a trivial solution $d_z(\mathbf{G})=0$. Unlike this, the transversal component $\mathbf{d}_\perp(\mathbf{G})$ satisfies the equation

$$\frac{\omega^2}{c^2}\mathbf{d}_\perp(\mathbf{G})=\sum_{\mathbf{G}'}\eta(\mathbf{G}-\mathbf{G}')[(k^2+G^2)\mathbf{d}_\perp(\mathbf{G}')-\mathbf{G}\mathbf{G}\cdot\mathbf{d}_\perp(\mathbf{G}')-\mathbf{G}kd_z(\mathbf{G}')]. \tag{57}$$

It has a nontrivial solution $\mathbf{d}_\perp^{(0)}(\mathbf{G})$ in the static limit. Namely, in this limit Eq. (57) takes the form

$$\sum_{\mathbf{G}'}\eta(\mathbf{G}-\mathbf{G}')[G^2\mathbf{d}_\perp^{(0)}(\mathbf{G}')-\mathbf{G}\mathbf{G}\cdot\mathbf{d}_\perp^{(0)}(\mathbf{G}')]\equiv-\sum_{\mathbf{G}'}\eta(\mathbf{G}-\mathbf{G}')\mathbf{G}\times[\mathbf{G}\times\mathbf{d}_\perp^{(0)}(\mathbf{G}')]=0. \tag{58}$$

This equation is satisfied if

$$\sum_{\mathbf{G}'}\eta(\mathbf{G}-\mathbf{G}')\mathbf{d}_\perp^{(0)}(\mathbf{G}')=\mathbf{G}\beta(\mathbf{G}),\quad \mathbf{G}\neq 0, \tag{59}$$

where $\beta(\mathbf{G})$ is an arbitrary function. Note that the Fourier components of the displacement $\mathbf{d}_\mathbf{k}(\mathbf{G})$ and the electric $\mathbf{e}_\mathbf{k}(\mathbf{G})$ fields are related as

$$\mathbf{e}_\mathbf{k}(\mathbf{G})=\sum_{\mathbf{G}'}\eta(\mathbf{G}-\mathbf{G}')\mathbf{d}_\mathbf{k}(\mathbf{G}'),$$

$$\mathbf{d}_\mathbf{k}(\mathbf{G})=\sum_{\mathbf{G}'}\varepsilon(\mathbf{G}-\mathbf{G}')\mathbf{e}_\mathbf{k}(\mathbf{G}'). \tag{60}$$

The first of these equations implies that the left-hand side of Eq. (59) is equal to $\mathbf{e}_\perp^{(0)}(\mathbf{G})$. Then, by the same equation, $\mathbf{G}\times\mathbf{e}_\perp^{(0)}(\mathbf{G})=0$. In view of this relation, Eq. (59) is equivalent to the electrostatic condition $\nabla\times\mathbf{E}=0$. The existence of a nontrivial solution of Eq. (57) means that the expansion of the longitudinal component $d_z(\mathbf{G})$ in the low-frequency limit starts from higher orders of k than the expansion of the transversal component $\mathbf{d}_\perp(\mathbf{G})$. In other words, Eq. (55) in the low-frequency limit has a solution in the form of a pure transversal wave ($D_z=0$) that is the necessary condition for homogenization. This is also obvious from applying the index ellipsoid to the problem at hand.

When the wave propagates along the cylinders, the in-plane inhomogeneities are not averaged out over many wavelengths, as occurs for oblique or in-plane propagation. Because of this ''lack of averaging,'' the solution of the wave equation in the low-frequency limit is not a pure plane wave but it exhibits a periodic dependence on the in-plane coordinates x and y,

$$\mathbf{D}(\mathbf{r}) \to_{k\to 0} \exp(ikz) \sum_{\mathbf{G}'} \mathbf{d}_{\perp}^{(0)}(\mathbf{G}') \exp(iG'_x x + iG'_y y). \tag{61}$$

It is important to note that, unlike the general case of (off-axis) propagation[35] [see Eq. (8) and below] here the nonzero harmonics $\mathbf{d}_{\perp}^{(0)}(\mathbf{G}\neq 0)$ are *not* much smaller than the $\mathbf{G}=0$ harmonic. As a matter of fact, we will prove [see Eq. (66)] that these harmonics are of the same order in k. This explains why Eq. (61) does not simplify in the long-wavelength limit, with the consequence that the wave fronts are *not* plane. Evidently, the cases of oblique and, especially, in-plane propagation are favorable for homogenization because the wavelength $2\pi/k$ covers an infinite number of unit cells. This, however, is not the case for on-axis propagation.

It is interesting to consider the behavior of the **H** and **E** fields as well, for $\mathbf{k}\|\hat{\mathbf{z}}$. As we have seen in Sec. II [see Eq. (10)) below], it follows from Maxwell's equations that $\mathbf{D}(\mathbf{r})=\sqrt{\varepsilon_{eff}}\mathbf{H}(\mathbf{r})\times\hat{\mathbf{k}}$ and $\mathbf{H}(\mathbf{r})=\sqrt{\varepsilon_{eff}}\hat{\mathbf{k}}\times\mathbf{E}(\mathbf{r})$. We just found that, for propagation along the cylinders, the **D** wave is not plane; then the linearity of Maxwell's equations implies that $\mathbf{D}(\mathbf{r})$ and $\mathbf{H}(\mathbf{r})$ are not plane either. Indeed, the wave fronts of all the fields are rippled in the $x-y$ plane, the structure of the ripples being periodic—with the periodicity of the 2D lattice. The mathematical reason for the planes of constant phase having this periodicity is that the amplitudes of all the *partial* plane waves with $k\hat{\mathbf{z}}+\mathbf{G}$ are all of the same order in k. From the formulas above we see that $\mathbf{H}(\mathbf{r})$, as well as $\mathbf{D}(\mathbf{r})$, is a transverse wave. The polarization of the $\mathbf{E}(\mathbf{r})$ field can be *hopefully* deduced from the index ellipsoid, Fig. 1. (Properly, it should be determined from the solution of the eigenvalue problem for the electric field which we did not undertake.) For on-axis propagation, the displacement vectors $\mathbf{D}(\mathbf{r})$ of the two modes are parallel to the x_0 and y_0 axes of the index ellipsoid. We recall from crystal optics[3,38] [also see just before Eq. (40)] that whenever **D** is parallel to one of the principal axes then $\mathbf{E}\|\mathbf{D}$. The conclusion then is that the electric field is also a transverse wave.

Needless to say, the optical (long-wavelength) modes that propagate in natural crystals are plane waves—for *any* propagation direction. This is also true for 3D photonic crystals.[29] As we have just found out, the eigenmodes of a 2D photonic crystal that propagate parallel to the cylinders are not plane waves, but have periodically rippled wave fronts. In this aspect, then, 2D photonic crystals differ qualitatively from their three-dimensional counterparts and from natural crystals. We are aware of only one other situation, where the equiphase surfaces are periodic, namely propagation in a 1D photonic crystal (superlattice) in a direction that is parallel to the interfaces.

In the 1D case it turns out that the forms of the homogenized fields are different for the ordinary (TE) and extraordinary (TM) waves. In the ordinary wave the electric field $\mathbf{E}_{\mathbf{k}}(\mathbf{r})$ is parallel to the interfaces and therefore it is a *continuous* function of the coordinates at any frequency. In the low-frequency limit this field is expanded over kd (d is the period), and the zero-order term gives the homogenized plane-wave solution. (This is true, of course, for any direction of propagation.) At the same time the spatial distribution of the displacement field $\mathbf{D}_{\mathbf{k}}(\mathbf{r})$ [which is parallel to $\mathbf{E}_{\mathbf{k}}(\mathbf{r})$] is not homogeneous along the superlattice axis. This field exhibits a periodic dependence in the axial direction (i.e., it is not a plane wave) and it is concentrated in the high-ε regions.[42] Unlike this, the electric field of the extraordinary wave [with $\mathbf{H}_{\mathbf{k}}(\mathbf{r})$ parallel to the interfaces] has a component perpendicular to the interfaces, $\mathbf{E}_n(\mathbf{r})$. This component satisfies the equation $D_n(\mathbf{r})=\varepsilon(\mathbf{r})E_n(\mathbf{r})=\text{const}$. Then for any frequency and direction of propagation the spatial dependence of $E_n(\mathbf{r})$ follows the periodicity of the lattice. For any direction except propagation along the layers this component turns out to be small (when $k\to 0$) as compared with the component parallel to the interfaces. Therefore the electric field is almost a plane wave in the low-frequency limit. However, for propagation parallel to the layers these two components are of the same order of magnitude. In this case the electric field (and, because of the linearity of Maxwell's equations, also the magnetic and the displacement fields) is *not* a plane wave. Hence the method of the index ellipsoid is not applicable (as we have also seen for 2D photonic crystals).

The effective dielectric constant Eq. (10) is obtained from the condition that the set of coupled homogeneous equations (56) and (57) has a nontrivial solution. In order to decouple these equations we use the transversality of the displacement field,

$$(\mathbf{k}+\mathbf{G})\cdot\mathbf{d}_{\mathbf{k}}(\mathbf{G}) = kd_z + \mathbf{G}\cdot\mathbf{d}_{\perp}(\mathbf{G}) = 0. \tag{62}$$

Substituting $kd_z=-\mathbf{G}\cdot\mathbf{d}_{\perp}(\mathbf{G})$ into Eq. (57), we get an equation which contains only $\mathbf{d}_{\perp}(\mathbf{G})$,

$$\frac{\omega^2}{c^2}\mathbf{d}_{\perp}(\mathbf{G}) = \sum_{\mathbf{G}'} \eta(\mathbf{G}-\mathbf{G}')[(k^2+G^2)\mathbf{d}_{\perp}(\mathbf{G}') - \mathbf{G}\mathbf{G}\cdot\mathbf{d}_{\perp}(\mathbf{G}') + \mathbf{G}\mathbf{G}'\cdot\mathbf{d}_{\perp}(\mathbf{G}')]. \tag{63}$$

Since this equation is even with respect to substitution $k\to -k$, the function $\mathbf{d}_{\perp}(\mathbf{G})$ may be expanded in even powers of k. The zero-order term for the Fourier components with $\mathbf{G}\neq 0$ may be obtained from Eq. (58). The term $\mathbf{d}_{\perp}^{(0)}(\mathbf{G}=0)$ which enters into Eq. (61) is calculated directly from Eq. (57). For $\mathbf{G}=0$ this equation takes the form

$$\frac{\omega^2}{c^2}\mathbf{d}_{\perp}(0) = k^2 \sum_{\mathbf{G}'} \eta(-\mathbf{G}')\mathbf{d}_{\perp}(\mathbf{G}') = k^2\mathbf{e}_{\perp}(0). \tag{64}$$

The last equality relies on the first of the identities (60). Taking the limit $\omega,k\to 0$ and using Eq. (10) we obtain the relation between static components of the electric and displacement field,

$$\mathbf{d}_{\perp}^{(0)}(0) = \varepsilon_{eff}\mathbf{e}_{\perp}^{(0)}(0), \tag{65}$$

which, in fact, is the electrostatic definition of $\boldsymbol{\epsilon}_{eff}$ since it relates the mean values of the electric and the displacement fields. While this definition involves only the $\mathbf{G}=0$ components (the mean values), the component $\mathbf{d}_{\perp}^{(0)}(0)$ is expressed

through all the other components $\mathbf{d}_\perp^{(0)}(\mathbf{G}\neq 0)$ by susbstitution of Eq. (60) into the right-hand side of Eq. (65),

$$\mathbf{d}_\perp^{(0)}(0)=\frac{1}{\varepsilon_{eff}^{-1}-\overline{\eta}}\sum_{\mathbf{G}'\neq 0}\eta(-\mathbf{G}')\mathbf{d}_\perp^{(0)}(\mathbf{G}'). \tag{66}$$

In Eq. (59) we separate the term with $\mathbf{G}'=0$ and substituting $\mathbf{d}_\perp^{(0)}(0)$ from Eq. (66) we obtain an infinite set of linear equations for $\mathbf{d}_\perp^{(0)}(\mathbf{G})$,

$$\sum_{\mathbf{G}'\neq 0}\left[\eta(\mathbf{G}-\mathbf{G}')+\frac{1}{\varepsilon_{eff}^{-1}-\overline{\eta}}\eta(\mathbf{G})\,\eta(-\mathbf{G}')\right]\mathbf{d}_\perp^{(0)}(\mathbf{G}') =\mathbf{G}\beta(\mathbf{G}). \tag{67}$$

The component $\mathbf{d}_\perp^{(0)}(\mathbf{G})$ corresponds to the static limit. According to Eq. (62) $\mathbf{G}\cdot\mathbf{d}_\perp^{(0)}(\mathbf{G})=0$. This condition gives the polarization of the displacement field $\mathbf{d}_\perp^{(0)}(\mathbf{G})$ along the unit vector $\mathbf{n}_2(\mathbf{G})$ [see Eq. (19)]. Taking the projection of Eq. (67) on $\mathbf{n}_2(\mathbf{G})$ we get an infinite set of homogeneous equations for the scalars $d_\perp^{(0)}(\mathbf{G})$,

$$\sum_{\mathbf{G}'\neq 0}\cos(\mathbf{G},\mathbf{G}')[(\varepsilon_{eff}^{-1}-\overline{\eta})\,\eta(\mathbf{G}-\mathbf{G}') +\eta(\mathbf{G})\,\eta(-\mathbf{G}')]d_\perp^{(0)}(\mathbf{G}')=0. \tag{68}$$

Here we used that $\mathbf{n}_2(\mathbf{G})\cdot\mathbf{n}_2(\mathbf{G}')=\mathbf{G}\cdot\mathbf{G}'/GG' =\cos(\mathbf{G},\mathbf{G}')$.

Equation (68) has nontrivial solutions if

$$\det_{\mathbf{G},\mathbf{G}'\neq 0}\{\mathbf{G}\cdot\mathbf{G}'[(\varepsilon_{eff}^{-1}-\overline{\eta})\,\eta(\mathbf{G}-\mathbf{G}')+\eta(\mathbf{G})\,\eta(-\mathbf{G}')]\} =0. \tag{69}$$

The set of linear equations (55) for $\mathbf{d_k}(\mathbf{G})$ has two solutions, corresponding to two orthogonal polarizations of the propagating mode. In the low-frequency limit this set has been reduced to Eq. (68). The latter thus must also have two solutions. To obtain these, we follow the same method as was used to solve Eqs. (23). First we multiply Eq. (69) by $\det\{[\mathbf{G}\cdot\mathbf{G}'\,\eta(\mathbf{G}-\mathbf{G}')]^{-1}\}$ and get a standard eigenvalue problem in the form of Eq. (34), where the matrix $B(\mathbf{G},\mathbf{G}')$ is replaced by

$$D(\mathbf{G},\mathbf{G}')=-\eta(\mathbf{G})\sum_{\mathbf{G}''\neq 0}\mathbf{G}\cdot\mathbf{G}''\,\eta(-\mathbf{G}'') \times[\mathbf{G}''\cdot\mathbf{G}'\,\eta(\mathbf{G}''-\mathbf{G}')]^{-1},\quad \mathbf{G},\mathbf{G}'\neq 0. \tag{70}$$

Even though the matrix $D(\mathbf{G},\mathbf{G}')$ looks quite similar to the matrix $B(\mathbf{G},\mathbf{G}')$ given by Eq. (35), the former *cannot* be written as a product of two factors, one of which depends only on $\mathbf{G}$ and the other only on $\mathbf{G}'$. Nevertheless, due to the factor $\mathbf{G}\cdot\mathbf{G}''$ each element of the matrix $D(\mathbf{G},\mathbf{G}')$ can be represented as a sum of such products,

$$D(\mathbf{G},\mathbf{G}')=-\eta(\mathbf{G})[G_x b_x(\mathbf{G}')+G_y b_y(\mathbf{G}')], \tag{71}$$

where

$$b_i(\mathbf{G})=\sum_{\mathbf{G}'\neq 0}G_i'\,\eta(-\mathbf{G}')[\mathbf{G}\cdot\mathbf{G}'\,\eta(\mathbf{G}'-\mathbf{G})]^{-1},\quad i=x,y. \tag{72}$$

For the matrix $D(\mathbf{G},\mathbf{G}')$, the coefficients α_n of the characteristic polynomial [see Eq. (27)] can be obtained via the recursive relation (29), with the matrix C replaced by the matrix D. Since Eq. (30) is not valid for the matrix D, the coefficient α_2 does not vanish. Instead, it can be shown after simple, but rather long algebra that the next coefficient, α_3, vanishes,

$$\alpha_3=-\frac{1}{3}[\mathrm{Tr}(D^3)+\alpha_1\mathrm{Tr}(D^2)+\alpha_2\mathrm{Tr}D] =-\frac{1}{3}\left[\mathrm{Tr}(D^3)-\frac{3}{2}\mathrm{Tr}\,D\,\mathrm{Tr}(D^2)+\frac{1}{2}(\mathrm{Tr}\,D)^3\right]=0, \tag{73}$$

for any matrix represented in the form (71). All subsequent coefficients α_n with $n=4,5,\ldots$ also vanish due to the generalized version of the property (73),

$$\alpha_n=-\frac{1}{n}[\mathrm{Tr}(D^n)+\alpha_1\mathrm{Tr}(D^{n-1})+\alpha_2\mathrm{Tr}(D)^{n-2}]=0, \tag{74}$$

that follows from Eq. (73) by mathematical induction. Now the characteristic equation (34), with the matrix $B(\mathbf{G},\mathbf{G}')$ replaced by $D(\mathbf{G},\mathbf{G}')$, is reduced to a simple quadratic equation,

$$\det_{\mathbf{G},\mathbf{G}'\neq 0}[D(\mathbf{G},\mathbf{G}')-\Lambda\,\delta_{\mathbf{G}\mathbf{G}'}] =\lim_{n\to\infty}(-1)^n\Lambda^{n-2}(\Lambda^2+\alpha_1\Lambda+\alpha_2)=0. \tag{75}$$

Two roots of this equation, $\Lambda_{1,2}$, give the two principal dielectric constants

$$\varepsilon_{1,2}=\frac{1}{(\overline{\eta}+\Lambda_{1,2})}=\left\{\overline{\eta}+\frac{1}{2}\mathrm{Tr}D\pm\frac{1}{2}\sqrt{2\,\mathrm{Tr}(D)^2-(\mathrm{Tr}\,D)^2}\right\}^{-1}. \tag{76}$$

There is no correspondence between the order of the indices 1,2 and the $\pm$ signs in Eq. (76).

In Sec. III we derived the formulas (44) and (45) for $\varepsilon_{1,2}$ considering in-plane propagation. Equation (76) is based on the analysis of the wave equation for the case of propagation parallel to the cylinders. These two approaches must give the same results for the principal dielectric constants, that is, the right-hand sides of Eqs. (44) and (45), and Eq. (76), must be identically equal. In the next section we will prove this analytically for the case of a rectangular lattice. The proof for an arbitrary (oblique) lattice is too long and cumbersome; it is much easier to verify the equivalence numerically.

Each of the representations for the principal dielectric constants possesses definite advantages. If the symmetry of the crystal is rather high and the axes of the index ellipsoid are aligned with crystallographic axes, it is easier to calculate $\varepsilon_{1,2}$ using the Eqs. (44) and (45). On the other hand, in the

asymmetric case Eq. (76) is preferable if one is interested only in the values of $\varepsilon_{1,2}$ but not in the orientation of the principal axes with respect to the crystallographic axes.

One more representation for the principal dielectric constants can be obtained if we replace the left-hand side of Eq. (59) by $\mathbf{e}_{\perp}^{(0)}(\mathbf{G})$ [see the first Eq. (60)]. The calculations using the E method are presented in Appendix C. Here we give the final solution for $\varepsilon_{1,2}$,

$$\varepsilon_{1,2}=\overline{\varepsilon}+\frac{1}{2}\mathrm{Tr}F\pm\frac{1}{2}\sqrt{2\,\mathrm{Tr}(F)^2-(\mathrm{Tr}\,F)^2}, \tag{77}$$

where the matrix $F(\mathbf{G},\mathbf{G}')$ is

$$F(\mathbf{G},\mathbf{G}')=-\varepsilon(\mathbf{G})\sum_{\mathbf{G}''\neq 0}\mathbf{G}\cdot\mathbf{G}''\varepsilon(-\mathbf{G}'') \times[\mathbf{G}''\cdot\mathbf{G}'\varepsilon(\mathbf{G}''-\mathbf{G}')]^{-1},\quad \mathbf{G},\mathbf{G}'\neq 0. \tag{78}$$

Note that the matrix $F(\mathbf{G},\mathbf{G}')$ has the same structure as the matrix $D(\mathbf{G},\mathbf{G}')$ with $\eta(\mathbf{G})$ replaced by $\varepsilon(\mathbf{G})$. The representation (78) must be equivalent to Eq. (76) [and to Eqs. (44) and (45)] for an infinite number of plane waves ($\mathbf{G}$ terms) in the summations. However, in the numerical calculations the matrices have to be cut to a finite size, of course, and that gives rise to convergence errors. In the next section we discuss the problem of convergence and give some practical recipes on how to increase the accuracy of the numerical results without increasing the number of plane waves involved in the calculations.

VII. 2D PHOTONIC CRYSTAL WITH RECTANGULAR LATTICE

A photonic crystal with a rectangular lattice is biaxial, i.e., the three principal dielectric constants are all different. This is true irrespective of the cross-sectional form of the cylinders. Thus this structure represents the general situation in crystal optics. At the same time, for this structure the calculations of $\varepsilon_{1,2}$ are simplified, essentially because the axes of the index ellipsoid are aligned with the crystallographic axes [the angle $\theta=0$ in Eq. (43)] and the unit cell possesses an inversion center, so that $\varepsilon(-\mathbf{G})=\varepsilon(\mathbf{G})$. The latter holds only if the inclusions have an axis of symmetry of the second order. For the rectangular lattice, the in-plane principal dielectric constants Eqs. (44) and (45) can be written compactly as

$$\varepsilon_{1,2}=\left\{\overline{\eta}-\sum_{\mathbf{G},\mathbf{G}'\neq 0}G_{y,x}G'_{y,x}\eta(\mathbf{G}) \times\eta(-\mathbf{G}')[\mathbf{G}\cdot\mathbf{G}'\eta(\mathbf{G}'-\mathbf{G})]^{-1}\right\}^{-1}. \tag{79}$$

Here $[\cdots]^{-1}$ implies matrix inversion, while $\{\cdots\}^{-1}$ means "reciprocal." First we demonstrate that the $\varepsilon_{1,2}$ as given by Eqs. (44), (45), and (76) are identical. It follows from the definitions of the matrices $D(\mathbf{G},\mathbf{G}')$, A_{xx} and A_{yy} [see Eqs. (39) and (70)] that $\mathrm{Tr}\,D=-(A_{xx}+A_{yy})$ for any lattice. Then a direct comparison of Eqs. (44), (45), and (76) shows that the different representations are identical if the following relation holds:

$$-A_{xx,yy}=-\frac{1}{2}(A_{xx}+A_{yy})\pm\sqrt{2\,\mathrm{Tr}(D^2)-(\mathrm{Tr}\,D)^2}. \tag{80}$$

The last equality leads to

$$A_{xx}^2+A_{yy}^2=\mathrm{Tr}(D^2), \tag{81}$$

as can be proved by the direct substitution of the matrix $D(\mathbf{G},\mathbf{G}')$ into Eq. (81). The corresponding calculations are given in Appendix D. The proof for the general 2D Bravais lattice follows a similar procedure, but the calculations are much more cumbersome.

The formulas (76) and (77) were obtained via the D and E methods, respectively. Their equivalency [as well as the equivalency of Eqs. (36) and (47)] is based on the fact that the solution of Maxwell's equations is unique and either of the vector functions, $\mathbf{H}(\mathbf{r})$, $\mathbf{E}(\mathbf{r})$, or $\mathbf{D}(\mathbf{r})$, gives complete information about the spatial distribution of electromagnetic field. While this general statement is beyond doubt, a direct proof would be desirable. The equivalency of formulas (76) and (77) requires that

$$\left\{\overline{\eta}+\frac{1}{2}\mathrm{Tr}\,D\pm\frac{1}{2}\sqrt{2\,\mathrm{Tr}\,D^2-(\mathrm{Tr}\,D)^2}\right\}\left\{\overline{\varepsilon}+\frac{1}{2}\mathrm{Tr}\,F \pm\frac{1}{2}\sqrt{2\,\mathrm{Tr}\,F^2-(\mathrm{Tr}\,F)^2}\right\}=1. \tag{82}$$

Unfortunately, we are unable to provide an analytic justification for this identity—even in the simple case of a square lattice of circular cylinders. For this uniaxial crystal the arguments of the square roots in Eq. (82) must vanish, so that Eq. (82) reduces to

$$\left(\overline{\eta}+\frac{1}{2}\mathrm{Tr}D\right)\left(\overline{\varepsilon}+\frac{1}{2}\mathrm{Tr}\,F\right)=1. \tag{83}$$

In Fig. 5 we give numerical evidence that the three representations of $\varepsilon_{1,2}$ discussed do converge to about the same value when the number of plane waves N ($\mathbf{G}$ values) is sufficiently large. In parts (a) and (b) we consider two mutually conjugate photonic crystals. In Fig. 5(a) we plot $\varepsilon_{1,2}(1/N)$ for a photonic crystal of circular Si cylinders ($\varepsilon_a=12.25$) placed in air ($\varepsilon_b=1$). The anisotropy of the lattice is specified by the ratio of the sides of the rectangle; in our case this ratio is 2:1. In Fig. 5(b) the same dependence is shown for air holes ($\varepsilon_a=1$) in Si host ($\varepsilon_b=12.25$). For both cases the filling fraction is $f=0.25$. The curves in Fig. 5 clearly demonstrate that when $1/N\to 0$ the effective dielectric constants given by Eqs. (76) and (77) converge to about the same value, namely $\varepsilon_1\approx 1.77$ and $\varepsilon_2\approx 1.42$ for Si cylinders in air, and $\varepsilon_1\approx 8.64$ and $\varepsilon_2\approx 6.92$ for air holes in Si. It is also worthwhile to note that numerical data for the effective dielectric constants given by Eqs. (44) and (45) coincide *exactly* with the ones given by Eq. (76) (squares in Fig. 5), thus

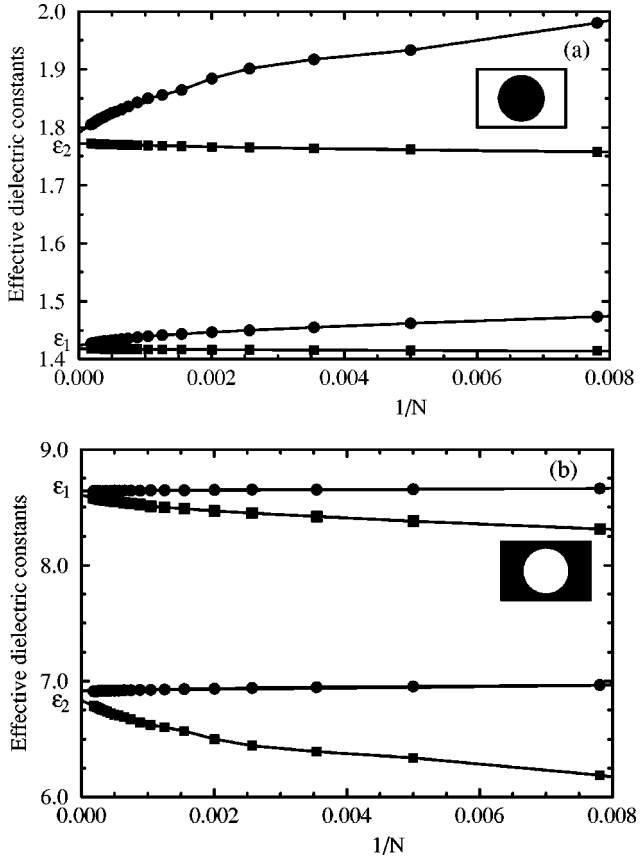

FIG. 5. Numerical evidence of the equivalence of the formulas (76) and (77) for a pair of conjugate photonic crystals with rectangular lattices. (a) Si cylinders in air and (b) air cylinders in a Si host. Squares and circles show the data obtained from Eqs. (76) and (77), respectively (the lines are guides to the eyes). The number of **G** values (plane waves) involved in the calculations ranges from 128 to 5314. Note that the principal dielectric constants ε_1 and ε_2 computed by the two methods converge to roughly the same values in the limit of a very large number N of plane waves. Nevertheless, the method based on Eq. (76) [(77)] converges much more rapidly for the material (air) cylinders.

demonstrating that the identity (81) is valid even for finite N. Note that both approaches are based on the η representation.

At the same time one can see that the rates of convergence are considerably different. For material cylinders the data obtained from Eq. (76) [squares in Fig. 5(a)] give much higher accuracy than the data obtained from Eq. (77) [circles in Fig. 5(a)] (for equal values of N). On the other hand, for air cylinders embedded in the material host [see Fig. 5(b)] the situation is just the opposite. We note that, for 3D photonic crystals with a simple-cubic lattice the ε representation (E method) also exhibits better convergence with the number of the plane waves if $\varepsilon_b > \varepsilon_a$.[43] This conclusion remains valid not only in the long-wavelength limit but at finite frequencies as well.[44] Note that, for any N, the ε representation [based on Eq. (77)] gives excessively large results for the principal dielectric constants, while the η representation [based on Eqs. (44), (45) or (76)] gives too small results.

If the dielectric contrast between the constituents of the photonic crystal increases, then the difference between the results obtained for finite N by the ϵ-representation and by the η representation becomes much greater. Since the computational effort grows very fast with the number N (it can hardly be larger than 8000), one obtains erroneous results if an improper method is used in the numerical simulations. In particular, from the discussion above it is obvious that the ε representation cannot be used to calculate the effective dielectric constants of a periodic array of perfectly conducting cylinders, $\varepsilon_a \to \infty$. In this limiting case $\bar{\varepsilon} = \infty$ and numerical results with *any finite number* of plane waves are incorrect. On the other hand, the η representation works perfectly well for arrays with $\varepsilon_a \gg 1$, leading to excellent agreement with results obtained from a direct solution of Poisson's equation.[45] The analysis of the case of perfectly conducting cylinders will be published elsewhere.[46]

For finite N the effective dielectric constants can be expanded in powers of $1/N$,

$$\varepsilon_{1,2}(N) = \varepsilon_{1,2}^{\infty} + \frac{a_{1,2}}{N} + \frac{b_{1,2}}{N^2}. \tag{84}$$

The parameters in this expansion are obtained numerically by fitting the curves in Fig. 5 to parabolas. They are given in Table I. These parameters are quantitative characteristics of the accuracy of the two different methods of calculations for $N > 10^3$. The smaller the absolute values of the coefficients $a_{1,2}$ and $b_{1,2}$ are for a given representation, the higher is its accuracy for a fixed value of N. Since these coefficients in the table differ by at least an order of magnitude, it is seen that the η (ε) representation is the right one to choose for material (air) cylinders—as concluded before. This recommendation can be reasonably extended to band-structure calculations for photonic crystals at finite frequencies.[44] Since the eigenvalue equation (6) for the magnetic field involves the Fourier coefficients $\eta(\mathbf{G})$ of the reciprocal dielectric

TABLE I. Parameters of parabolic fitting for the curves in Fig. 5, see Eq. (84).

	ε_1^{∞}	a_1	b_1	ε_2^{∞}	a_2	b_2
	Si cylinders in air ($\varepsilon_a = 12.25$, $\varepsilon_b = 1$)					
ε representation	1.789 93	86	−33 000	1.423 46	22	−8,100
η representation	1.772 24	−3	190	1.418 11	−0.9	50
	Air cylinders in Si host ($\varepsilon_a = 1$, $\varepsilon_b = 12.25$)					
ε representation	8.640 54	3	−12	6.917 18	6	−17
η representation	8.604 17	−130	38 500	6.836 48	−300	82 000

constant, this equation should be used if the inclusions of the photonic crystal are optically more dense than the host material. In the opposite case one should use the eigenvalue equation for the displacement vector, or the eigenvalue equation for the electric field, written in the ε representation.

The values of $\varepsilon_{1,2}^{\infty}$ in Table I were obtained by extrapolation to $N\to\infty$. The accuracy of these values can be estimated from Keller's theorem.[22] This theorem states that the principal dielectric constants for two conjugate composites that form a rectangular lattice satisfy the relation

$$r=\frac{\varepsilon_1(\varepsilon_a,\varepsilon_b)\varepsilon_2(\varepsilon_b,\varepsilon_a)}{\varepsilon_a\varepsilon_b}\equiv\frac{\varepsilon_2(\varepsilon_a,\varepsilon_b)\varepsilon_1(\varepsilon_b,\varepsilon_a)}{\varepsilon_a\varepsilon_b}\equiv 1. \tag{85}$$

Using the values of $\varepsilon_{1,2}^{\infty}$ in Table I we get two values [according to the two equalities in Eq. (85)] for the precision factors, namely $r=1.011$ and $r=1.004$, obtained from the ε-representation data. The same factors, calculated from the η-representation data, yield, $r=0.989$ and $r=0.996$. One can see that both methods give about the same relative error for r. This means that the extrapolation to $N=\infty$ washes out the difference between the accuracies of the two methods. Much higher accuracy is obtained if we use different representations for ε_1 and ε_2 in Eq. (85) , namely the η representation for Si cylinders and the ε representation for air cylinders. Substituting the corresponding data from Table I in Eq. (85) we get that $r=1.000\,73$ and $r=1.000\,26$. Thus by using ''the best'' representations for the effective dielectric constants much higher accuracy is obtained.

VIII. 2D PHOTONIC CRYSTAL WITH SQUARE LATTICE

This, of course, is a particular case of the previous section for the rectangular lattice, but, since it is one of the most common 2D photonic crystal structures, it deserves special attention. If the inclusions are circular cylinders of radius R the photonic crystal is uniaxial, so that $\varepsilon_H(\hat{\mathbf{k}})=\varepsilon_1=\varepsilon_2$ in Eq. (36) with ε_1 given by Eq. (46). We calculated the effective dielectric constant $\varepsilon=\varepsilon_1=\varepsilon_2$ for the same values of the parameters as before. In Fig. 6 we plot the dependence $\varepsilon(1/N)$ obtained from the η and ε representations for two conjugate structures. The two representations demonstrate a convergence to roughly the same value. As for the rectangular lattice, the $\eta(\varepsilon)$ representation converges faster for the structure with material (air) cylinders in the air (material) host. The square lattice possesses additional symmetry, of course, as compared with the rectangular lattice. In order to see the manifestation of the additional symmetry we represent the data of the fitting to parabolas in the following form.

Si cylinders:

$$\varepsilon=1.54738\left(1+\frac{23.3}{N}-\frac{7{,}755}{N^2}\right)\varepsilon \quad \text{representation,} \tag{86}$$

$$\varepsilon=1.53901\left(1-\frac{2.27}{N}+\frac{845}{N^2}\right)\eta \quad \text{representation.} \tag{87}$$

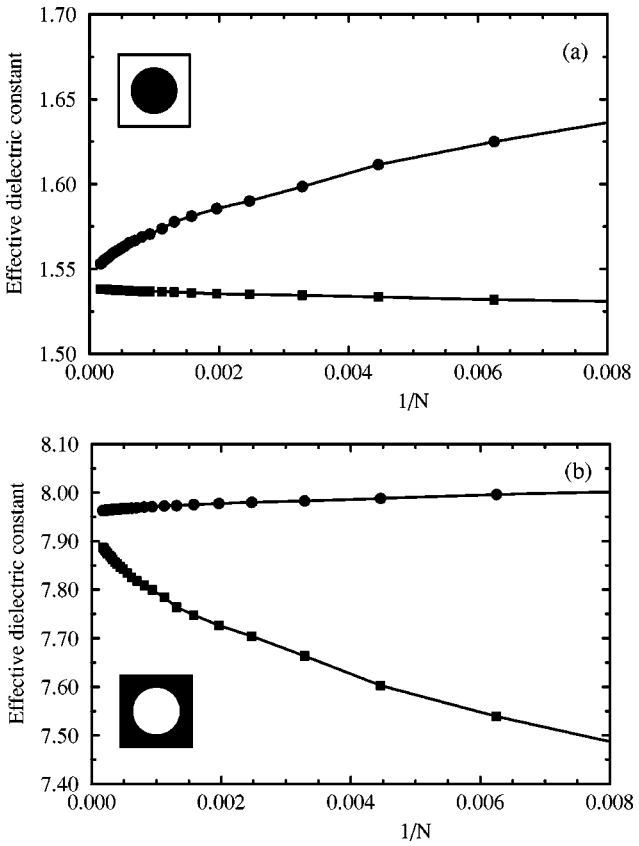

FIG. 6. The same as in Fig. 5 but for the square lattice. The photonic crystal is uniaxial therefore $\varepsilon_1=\varepsilon_2$. The number of **G** values (plane waves) involved in the calculations ranges from 24 to 5648. As in Fig. 5, for material (air) cylinders Eq. (76) [(77)] leads to much better convergence for the principal dielectric constant ε_1.

Air cylinders:

$$\varepsilon=7.95966\left(1+\frac{2.26}{N}-\frac{879}{N^2}\right)\varepsilon \quad \text{representation,} \tag{88}$$

$$\varepsilon=7.9165\left(1-\frac{23.1}{N}+\frac{7{,}870}{N^2}\right)\eta \quad \text{representation.} \tag{89}$$

These fitting formulas are valid for $N>10^3$. Note that the linear corrections in Eqs. (86) and (89) have opposite signs and almost equal absolute values. The same is true for Eqs. (87) and (88). The quadratic terms, essentially, also compensate each other. This leads to cancellations if Eqs. (87)–(88) are substituted into the precision factor Eq. (85). That is, r is calculated using the best representation for ε for each structure. We get that

$$r\cong 1.000\,00-\frac{39}{N^2}+O(N^{-3}). \tag{90}$$

Since the linear term is absent in this formula, the absolute numerical error for r is much smaller than that for the effective dielectric constant, even if calculated using the fastest converging representation. Therefore for a square lattice the

accuracy of the precision factor is much higher than that of the effective dielectric constant. At the same time, for a rectangular lattice the above mentioned cancellation does not occur, and Eq. (85) gives true information about the accuracy of numerical calculations.

IX. CONCLUSIONS

We have developed a comprehensive theory, in the long-wavelength limit, of photonic crystals with 2D periodicity. The homogenized composite has been characterized in the language of ''crystal optics,'' namely, the three principal dielectric constants, have been expressed in terms of the microstructure of the unit cell. Unlike most works in homogenization theory, our compact analytic formulas for the principal dielectric constants are very general: no limiting assumptions whatsoever have been made about the Bravais lattice, the cross-sectional form of the cylinders, the filling fraction of the constituents, the dielectric contrast, or the direction of propagation. A modest numerical effort (involving, essentially, only a matrix inversion) leads to high-precision results for the aforementioned dielectric constants. For dielectric cylinders in air the representation of choice should be based on the Fourier expansion of the reciprocal dielectric constant $\eta(\mathbf{r})=1/\varepsilon(\mathbf{r})$. On the other hand, for air cylinders in a dielectric background the Fourier expansion of the dielectric constant $\varepsilon(\mathbf{r})$ itself leads to much better convergence. It is worth noting that the acoustic band is frequently linear (to a reasonable approximation) up to frequencies approaching the lower edge of the photonic band gap. Thus the utility of our results may go beyond the nominal requirement that the Bloch wavelength is much greater than the period.

Our treatment of the optical constants—the principal dielectric constants ε_i and the effective dielectric constant $\varepsilon_{eff}(\hat{\mathbf{k}})$—has been formulated fully within the conceptual framework of crystal optics. The same is true for the fields—electric, magnetic, and displacement—with one notable exception, namely propagation parallel to the cylinders. Obviously, this direction stands out in the characterization of a 2D photonic crystal, and has no counterpart for natural crystals or for 3D photonic crystals. We found that the wavefronts of a wave that propagates along the cylinders are not plane, but periodically rippled, with the periodicity following the pattern of the 2D Bravais lattice. This is true irrespective of whether the photonic crystal is uniaxial or biaxial.

It is important that our formulas for the principal dielectric constants have direct analogies in other areas of transport properties of inhomogeneous media. Thus all the ε's may be replaced by the corresponding μ's, σ's, or K's, and one gets useful formulas for the effective static magnetic permeability, the conductivity, or the thermal conductivity, respectively. This statement rests on the assumption that the constituent materials of the composite are isotropic. The analogy is explained by the fact that, in the quasistatic limit, Maxwell's equations reduce to the electrostatic formulas $\nabla\cdot\mathbf{D}=0$, $\nabla\times\mathbf{E}=0$ along with the constitutive relation $\mathbf{D}=\varepsilon\mathbf{E}$; the basic equations of magnetostatics, electric transport, and heat transport have the very same structure.

A similar approach could lead to the homogenization of photonic crystals with magnetic properties, and of phononic (or acoustic) crystals. In the latter case the general theory is expected to be considerably more complicated on account of the existence of longitudinal, as well as transverse waves, and the coupling of these via the inhomogeneity. We expect that our results will also have implications for the homogenization of random composites.

ACKNOWLEDGMENTS

We wish to thank David Bergman for useful correspondence related to the second part of Sec. V. We also acknowledge the CONACyT Grant Nos. 32191-E and 33808-E.

APPENDIX A: PROOF OF EQ. (13)

We multiply Eq. (11) by $\overline{\eta}G^2$. Now the left-hand side can be rewritten in the form

$$\overline{\eta}G^2\mathbf{h}_{\mathbf{k}}(\mathbf{G})=-\eta(0)\mathbf{G}\times[\mathbf{G}\times\mathbf{h}_{\mathbf{k}}(\mathbf{G})], \tag{A1}$$

where we took into account the transversality of the magnetic field, Eq. (5). It is easy to see that the term which is excluded from the summation over $\mathbf{G}'$ on the right-hand side of Eq. (11) is just minus the right-hand side of Eq. (A1). Including this term in the summation we get

$$\eta(\mathbf{G})\mathbf{G}\times[\mathbf{k}\times\mathbf{h}_{\mathbf{k}}(0)]+\sum_{\mathbf{G}'\neq 0}\eta(\mathbf{G}-\mathbf{G}')\mathbf{G}\times[\mathbf{G}'\times\mathbf{h}_{\mathbf{k}}(\mathbf{G}')]=0. \tag{A2}$$

Next we substitute $\mathbf{h}_{\mathbf{k}}(0)$ from Eq. (11) into Eq. (A2). Since in both equations the Fourier coefficient $\mathbf{h}_{\mathbf{k}}(\mathbf{G}')$ enters in the combination $\mathbf{G}'\times\mathbf{h}_{\mathbf{k}}(\mathbf{G}')$, it is convenient to consider this product as a new variable, as defined in Eq. (12). After this substitution Eq. (13) is obtained.

APPENDIX B: PROOF OF EQ. (30)

The identity (30) is valid for any matrix with matrix elements represented in the multiplicative form Eq. (28). For such a matrix

$$\begin{aligned}\mathrm{Tr}(C^n)&=\sum_{\mathbf{G}_1,\mathbf{G}_2,\ldots,\mathbf{G}_n\neq 0}\eta(\mathbf{G}_1)\varepsilon(-\mathbf{G}_2)\eta(\mathbf{G}_2)\\&\quad\times\varepsilon(-\mathbf{G}_3)\cdots\eta(\mathbf{G}_n)\varepsilon(-\mathbf{G}_1)\\&=\sum_{\mathbf{G}_1\neq 0}\eta(\mathbf{G}_1)\varepsilon(-\mathbf{G}_1)\sum_{\mathbf{G}_2\neq 0}\eta(\mathbf{G}_2)\varepsilon(-\mathbf{G}_2)\cdots\\&\quad\times\sum_{\mathbf{G}_n\neq 0}\eta(\mathbf{G}_n)\varepsilon(-\mathbf{G}_n)=(\mathrm{Tr}\,C)^n.\end{aligned} \tag{B1}$$

For $n=2$ the identity (30) reads $\mathrm{Tr}(C^2)=(\mathrm{Tr}\,C)^2$. The latter is true by virtue of Eq. (B1). Then is clear that the coefficient α_2 in Eq. (29) is zero. Now, assuming that Eq. (30) is true, it is straightforward to demonstrate that it is also satisfied for n replaced by $(n+1)$, namely

$$\mathrm{Tr}(C^{n+1}) = (\mathrm{Tr}\, C)^{n+1} = (\mathrm{Tr}\, C)^n \mathrm{Tr}\, C = \mathrm{Tr}(C^n)\mathrm{Tr}\, C. \tag{B2}$$

Due to this property of the matrix C the coefficients $\alpha_3, \alpha_4, \ldots$ also vanish.

APPENDIX C: PROOF OF EQS. (77) AND (78)

Substituting the first linear relation (60) between the Fourier components of the electric and displacement fields in the left-hand side of Eq. (59) we get that

$$\mathbf{e}_\perp^{(0)}(\mathbf{G}) = \mathbf{G}\beta(\mathbf{G}), \mathbf{G} \neq 0. \tag{C1}$$

We substitute this formula into the transversality condition (62), written in terms of the electric field with the help of Eq. (60):

$$\begin{aligned}\mathbf{G}\cdot\mathbf{d}_\perp^{(0)}(\mathbf{G}) &= \sum_{\mathbf{G}'} \varepsilon(\mathbf{G}-\mathbf{G}')\mathbf{G}\cdot\mathbf{e}_\perp^{(0)}(\mathbf{G}') \\ &= \sum_{\mathbf{G}'\neq 0} \varepsilon(\mathbf{G}-\mathbf{G}')\mathbf{G}\cdot\mathbf{e}_\perp^{(0)}(\mathbf{G}') + \varepsilon(\mathbf{G})\mathbf{G}\cdot\mathbf{e}_\perp^{(0)}(0) \\ &= 0. \end{aligned} \tag{C2}$$

Then, with the help of Eq. (C1) we obtain that

$$\begin{aligned}\mathbf{G}\cdot\mathbf{d}_\perp^{(0)}(\mathbf{G}) &= \sum_{\mathbf{G}'\neq 0} \varepsilon(\mathbf{G}-\mathbf{G}')\mathbf{G}\cdot\mathbf{G}'\beta(\mathbf{G}') + \varepsilon(\mathbf{G})\mathbf{G}\cdot\mathbf{e}_\perp^{(0)}(0) \\ &= 0. \end{aligned} \tag{C3}$$

To get a closed set of linear equations for $\beta(\mathbf{G})$ we need to eliminate $\mathbf{e}_\perp^{(0)}(0)$ from Eq. (C3). First we express $\mathbf{e}_\perp^{(0)}(0)$ through all $\mathbf{e}_\perp^{(0)}(\mathbf{G})$ $(\mathbf{G}\neq 0)$, using the second of Eq. (60) taken at $\mathbf{G}=0$ and Eq. (65),

$$\mathbf{e}_\perp^{(0)}(0) = (\varepsilon_{eff} - \overline{\varepsilon})^{-1} \sum_{\mathbf{G}'\neq 0} \varepsilon(-\mathbf{G}')\mathbf{e}_\perp^{(0)}(\mathbf{G}'). \tag{C4}$$

Now, using Eq. (C1) and substituting Eq. (C4) into Eq. (C3) we get a set of linear homogeneous equations for the new scalar variables $B(\mathbf{G}) = G\beta(\mathbf{G})$,

$$\begin{aligned}\sum_{\mathbf{G}'\neq 0} \cos(\mathbf{G},\mathbf{G}')[(\varepsilon_{eff}-\overline{\varepsilon})\varepsilon(\mathbf{G}-\mathbf{G}') \\ + \varepsilon(\mathbf{G})\varepsilon(-\mathbf{G}')]B(\mathbf{G}') = 0. \end{aligned} \tag{C5}$$

This set of equations is analogous to Eq. (68). Therefore the derivation of Eq. (77) follows the same method as the derivation of Eq. (76), with the obvious replacements $\eta(\mathbf{G}) \to \varepsilon(\mathbf{G})$ and $(\varepsilon_{eff}^{-1} - \overline{\eta}) \to (\varepsilon_{eff} - \overline{\varepsilon})$. This then replaces $D(\mathbf{G},\mathbf{G}')$, Eq. (70), by $F(\mathbf{G},\mathbf{G}')$, Eq. (78). In the quadratic equation corresponding to Eq. (75), now $\Lambda = \varepsilon_{1,2} - \overline{\varepsilon}$, while α_1 and α_2 are still given by Eq. (29), however, with $C(\mathbf{G},\mathbf{G}')$ replaced by $F(\mathbf{G},\mathbf{G}')$. This results in Eq. (77).

APPENDIX D: PROOF OF EQ. (80)

Using the definition of matrix $D(\mathbf{G},\mathbf{G}')$, Eq. (70), we obtain for its square

$$\begin{aligned}D^2(\mathbf{G},\mathbf{G}') = \sum_{\mathbf{G}_1,\mathbf{G}_2,\mathbf{G}_3\neq 0} (\mathbf{G}\cdot\mathbf{G}_1)(\mathbf{G}_2\cdot\mathbf{G}_3)\,\eta(\mathbf{G})\,\eta(-\mathbf{G}_1) \\ \times \eta(\mathbf{G}_2)\,\eta(-\mathbf{G}_3)[\mathbf{G}_1\cdot\mathbf{G}_2\,\eta(\mathbf{G}_1-\mathbf{G}_2)]^{-1} \\ \times[\mathbf{G}_3\cdot\mathbf{G}'\,\eta(\mathbf{G}_3-\mathbf{G}')]^{-1}, \mathbf{G},\mathbf{G}' \neq 0. \end{aligned} \tag{D1}$$

The trace of the matrix D^2 is given by

$$\begin{aligned}\mathrm{Tr}(D^2) = \sum_{\mathbf{G}_1,\ldots,\mathbf{G}_4\neq 0} (G_{1x}G_{2x}G_{3x}G_{4x} + G_{1y}G_{2y}G_{3y}G_{4y} \\ + G_{1x}G_{2x}G_{3y}G_{4y} + G_{1y}G_{2y}G_{3x}G_{4x}) \\ \times \eta(\mathbf{G}_1)\,\eta(-\mathbf{G}_2)\,\eta(\mathbf{G}_3)\,\eta(-\mathbf{G}_4) \\ \times[\mathbf{G}_2\cdot\mathbf{G}_3\,\eta(\mathbf{G}_2-\mathbf{G}_3)]^{-1}[\mathbf{G}_4\cdot\mathbf{G}_1\,\eta(\mathbf{G}_4-\mathbf{G}_1)]^{-1}. \end{aligned} \tag{D2}$$

The first two terms in Eq. (D2) contain products of either only x or only y components of the reciprocal vectors. These two terms, respectively, are equal to A_{xx}^2 and A_{yy}^2 [see Eq. (39)]. The remaining two terms contain products of x and y components and they can be presented in the following form:

$$\begin{aligned}\mathrm{Tr}(D^2) = A_{xx}^2 + A_{yy}^2 + \left\{\sum_{\mathbf{G}_1,\mathbf{G}_4\neq 0} G_{1x}G_{4y}\,\eta(\mathbf{G}_1)\,\eta(-\mathbf{G}_4)[\mathbf{G}_4\cdot\mathbf{G}_1\,\eta(\mathbf{G}_4-\mathbf{G}_1)]^{-1}\right\}\left\{\sum_{\mathbf{G}_2,\mathbf{G}_3\neq 0} G_{2x}G_{3y}\,\eta(-\mathbf{G}_2)\,\eta(\mathbf{G}_3)\right. \\ \left.\times[\mathbf{G}_2\cdot\mathbf{G}_3\,\eta(\mathbf{G}_2-\mathbf{G}_3)]^{-1}\right\} + \left\{\sum_{\mathbf{G}_1,\mathbf{G}_4\neq 0} G_{1y}G_{4x}\,\eta(\mathbf{G}_1)\,\eta(-\mathbf{G}_4)[\mathbf{G}_4\cdot\mathbf{G}_1\,\eta(\mathbf{G}_4-\mathbf{G}_1)]^{-1}\right\} \\ \times\left\{\sum_{\mathbf{G}_2,\mathbf{G}_3\neq 0} G_{2y}G_{3x}\,\eta(-\mathbf{G}_2)\,\eta(\mathbf{G}_3)[\mathbf{G}_2\cdot\mathbf{G}_3\,\eta(\mathbf{G}_2-\mathbf{G}_3)]^{-1}\right\}. \end{aligned} \tag{D3}$$

Each term in curly brackets is identically zero. To see this one needs to change the indices of summation. For example, upon changing $G_{1x} \to -G_{1x}, G_{4x} \to -G_{4x}$ the Fourier coefficients $\eta(\mathbf{G}_4-\mathbf{G}_1)$, $\eta(\mathbf{G}_1)$, and $\eta(-\mathbf{G}_4)$ in the first curly brackets remain unchanged due to the central symmetry of the unit cell. It is clear that the scalar product $\mathbf{G}_4\cdot\mathbf{G}_1$ is unchanged as well. At the same time the factor G_{1x} changes its sign, thus leading to the change of the sign of the whole expression in brackets. But since the change of dummy indices cannot change the value of the expression, it must be identically zero. This completes the proof of the identity Eq. (81) for a rectangular lattice.

[1] S.-Y. Lin, V. M. Hietala, L. Wang, and E. D. Jones, Opt. Lett. **21**, 1771 (1996).
[2] H. Kosaka, T. Kawashima, A. Tomita, M. Notomi, T. Tamamura, T. Sato, and S. Kawakami, Phys. Rev. B **58**, R10 096 (1998).
[3] M. Born and E. Wolf, *Principles of Optics* (Pergamon Press, Oxford, 1975).
[4] J. C. Maxwell-Garnett, Philos. Trans. R. Soc. London, Ser. A **203**, 385 (1904).
[5] W. Lamb, D. M. Wood, and N. W. Ashcroft, Phys. Rev. B **21**, 2248 (1980).
[6] K. Busch and C. M. Soukoulis, Phys. Rev. Lett. **75**, 3442 (1995).
[7] K. Busch and C. M. Soukoulis, Phys. Rev. B **54**, 893 (1996).
[8] D. Felbacq and G. Bouchitté, Waves Random Media **7**, 245 (1997).
[9] F. J. Garciá-Vidal, J. M. Pitarke, and J. B. Pendry, Phys. Rev. Lett. **78**, 4289 (1997).
[10] A. Kirchner, K. Busch, and C. M. Soukoulis, Phys. Rev. B **57**, 277 (1998).
[11] G. Guida, D. Maystre, G. Tayeb, and P. Vincent, J. Opt. Soc. Am. B **15**, 2308 (1998).
[12] W. I. Perrins, D. R. McKenzie, and R. C. McPhedran, Proc. R. Soc. London, Ser. A **369**, 207 (1979).
[13] G. W. Milton, R. C. McPhedran, and D. R. McKenzie, Appl. Phys. **25**, 23 (1981).
[14] L. C. Shen, C. Lui, J. Korringa, and K. J. Dunn, J. Appl. Phys. **67**, 7071 (1990).
[15] D. J. Bergman and K. J. Dunn, Phys. Rev. B **45**, 13 262 (1992).
[16] N. A. Nicorovici, R. C. McPhedran, and L. C. Botten, Phys. Rev. Lett. **75**, 1507 (1995).
[17] N. A. Nicorovici and R. C. McPhedran, Phys. Rev. E **54**, 1945 (1996).
[18] R. C. McPhedran, N. A. Nicorovici, and L. C. Botten, J. Electromagn. Waves Appl. **11**, 981 (1997).
[19] P. Lalanne, Appl. Opt. **35**, 5369 (1996); Phys. Rev. B **58**, 9801 (1998).
[20] Z. Hashin and S. Shtrickman, J. Appl. Phys. **33**, 3125 (1962).
[21] S. R. Coriell and J. L. Jackson, J. Appl. Phys. **39**, 4733 (1968).
[22] J. B. Keller, J. Math. Phys. **5**, 548 (1964).
[23] J. Nevard and J. B. Keller, J. Math. Phys. **6**, 2761 (1985).
[24] R. Fuchs, Phys. Rev. B **11**, 1732 (1975); D. J. Bergman, *ibid.* **14**, 4304 (1976); R. Fuchs and F. Claro, *ibid.* **39**, 3875 (1989).
[25] S. M. Rytov, Zh. Eksp. Teor. Fiz. **29**, 605 (1995) [JETP **2**, 466 (1956)]; P. Yeh, A. Yariv, and C.-S. Hong, J. Opt. Soc. Am. **67**, 423 (1977); R. C. McPhedran, L. C. Botten, M. S. Craig, M. Neviere, and D. Maystre, Opt. Acta **29**, 289 (1982).
[26] P. Yeh, *Optical Waves in Layered Media* (Wiley, New York, 1988).
[27] R. de Kronig and W. G. Penney, Proc. R. Soc. London, Ser. A **130**, 499 (1931).
[28] R. Tao, Z. Chen, and P. Sheng, Phys. Rev. B **41**, 2417 (1990).
[29] S. Datta, C. T. Chan, K. M. Ho, and C. M. Soukoulis, Phys. Rev. B **48**, 14 936 (1993).
[30] K. Ohtaka, T. Ueta, and Y. Tanabe, J. Phys. Soc. Jpn. **65**, 3068 (1996).
[31] A. A. Krokhin, J. Arriaga, and P. Halevi, Physica A **241**, 52 (1997).
[32] P. Halevi, A. A. Krokhin, and J. Arriaga, Phys. Rev. Lett. **82**, 719 (1999).
[33] P. Halevi, A. A. Krokhin, and J. Arriaga, Appl. Phys. Lett. **75**, 2725 (1999).
[34] G. W. Milton, R. C. McPhedran, and D. R. McKenzie, Appl. Phys. **25**, 23 (1981).
[35] Equation (9) fails for propagation parallel to the cylinders . In this case the double cross product in Eq. (8) is reduced to $\mathbf{G}'\mathbf{k}\cdot\mathbf{h}_{\mathbf{k}}(\mathbf{G}')$. This vector lies in the plane of periodicity and depends only on the field component parallel to the cylinders. Thus Eq. (8) is a relation between the in-plane component of $\mathbf{h}_{\mathbf{k}}(\mathbf{G}=0)$ and the parallel (z) components with all $\mathbf{G}$'s. Then we can only conclude that the parallel components approach zero at higher rates than the in-plane component $\mathbf{h}_{\mathbf{k}}(\mathbf{G}=0)$. This, however, does not mean that the in-plane components of $\mathbf{h}_{\mathbf{k}}(\mathbf{G}\neq 0)$ are much smaller than the in-plane component of $\mathbf{h}_{\mathbf{k}}(\mathbf{G}=0)$. Therefore, for $\mathbf{k}\|\hat{\mathbf{z}}$, Eq. (4) does not reduce to Eq. (9). In Sec. VI we consider the case of propagation parallel to the cylinders and show that all in-plane components of $\mathbf{d}_{\mathbf{k}}(\mathbf{G})$ approach zero with the same rate. This conclusion is also true for the in-plane components of $\mathbf{h}_{\mathbf{k}}(\mathbf{G})$.
[36] M. Plihal and A. A. Maradudin, Phys. Rev. B **44**, 8565 (1991).
[37] D. V. Beklemishev, *Dopolnitelnye Glavy Lineinoii Algebry* (Nauka, Moscow, 1983), p. 328 (in Russian).
[38] L. D. Landau, E. M. Lifshitz, and L. P. Pitaevskii, *Electrodynamics of Continuous Media*, 2nd ed. (Pergamon, Oxford, 1984).
[39] O. Wiener, Abh. Sachs. Akad. Wiss. Leipzig Math.-Naturwiss. Kl. **32**, 509 (1912).
[40] I. H. H. Zabel and D. Stroud, Phys. Rev. B **48**, 5004 (1993).
[41] We are thankful to D. Bergman who called our attention to this fact.
[42] J. D. Joannopoulos, R. D. Meade, and J. N. Winn, *Photonic Crystals: Molding the Flow of Light* (Princeton University Press, New Jersey, 1995).
[43] H.-S. Sözüer and J. Haus, J. Opt. Soc. Am. B **10**, 296 (1993).
[44] Z. Yuan and J. Haus, Opt. Express **3**, 19 (1998).
[45] P. Halevi, A. A. Krokhin, and J. Arriaga, Phys. Rev. Lett. **86**, 3211 (2001).
[46] A. A. Krokhin, P. Halevi, and J. Arriaga (unpublished).